Available online at www.sciencedirect.com
SCIENCE DIRECT®
Journal of Power Sources 147 (2005) 8–31
JOURNAL OF POWER SOURCES
www.elsevier.com/locate/jpowsour

Theoretical analysis of the role of interfaces in transport through oxygen ion and electron conducting membranes

Anil V. Virkar*

Department of Materials Science and Engineering, 122 South Central Campus Drive, University of Utah, Salt Lake City, UT 84112, USA

Received 22 December 2004; accepted 17 January 2005
Available online 6 April 2005

Abstract

This manuscript examines transport through oxygen ion and electronic conducting membranes including electrode/membrane interfaces by explicitly incorporating both ionic and electronic transport through the membranes and across interfaces. Spatial variation of electrochemical potential of oxygen ions, $\tilde{\mu}_{O^{2-}}$, electrochemical potential of electrons, $\tilde{\mu}_e$ (or reduced negative electrochemical potential of electrons, $\varphi = -\tilde{\mu}_e/e$, where e is the electronic charge), and chemical potential of molecular oxygen, μ_{O_2}, through membrane and across interfaces are examined as functions of transport properties of membranes and interfacial regions. The analysis shows that description of transport across electrode/membrane interfaces requires two transport parameters—one for ions, and the other for electrons. The transport equations are applied to fuel cells, pressure-driven oxygen separation through mixed ionic–electronic conducting (MIEC) membranes, and voltage-driven oxygen separation through predominantly oxygen ion conducting membranes. In fuel cells and MIEC oxygen separation membranes, the μ_{O_2} varies monotonically between the two end values corresponding to those at the two electrodes. Thus, in fuel cells and MIEC oxygen separation membranes, the stability of the membrane is assured as long as the oxygen partial pressure, p_{O_2}, on the fuel side or the permeate side is above the decomposition oxygen partial pressure of the membrane. By contrast, in voltage-driven oxygen separation membranes, μ_{O_2} in the membrane can lie outside of the end values. Thus, in the case of oxygen separation under an applied voltage, the transport properties of the material and the interfaces determine membrane stability. Implications of the analysis concerning the applicability of the so-called the three-electrode system under an applied voltage to investigate electrode polarization are presented. It is shown that the use of the three-electrode system for the estimation of electrode kinetics can lead to significant errors at high applied voltages, and may result in overestimation of electrocatalytic activity of the electrode. This manuscript also defines electrode overpotential in terms of the rate of potential useful work degraded as an irreversible process at an electrode and the net current measured in the external circuit. The as-defined overpotential may not be experimentally measurable.

Keywords: Mixed ion–electronic conductors; Oxygen ion conductors; Fuel cells; Oxygen separation; Transport across interfaces

1. Introduction

Many oxides transport both ionic (cationic and/or anionic) and electronic species. Of particular interest for applications such as fuel cells, water electrolysis, potentiometric oxygen sensors, oxygen separation under an applied voltage, etc. are materials, which can predominantly transport oxygen ions. For oxygen separation from air under an applied pressure gradient, materials, which exhibit significant transport of both oxygen ions and electronic defects, are of interest. Such materials are known as mixed ionic–electronic conductors (MIEC). Transport in oxygen ion conductors or in MIEC materials can be described by phenomenological equations, which have been well established for over 50 years [1–5]. Several published works have applied these transport equations for investigating ionic and electronic transport through membranes [6–11]. In most of these studies, the focus was on transport through membranes with emphasis on the role of defect chemistry, but rarely on the role of interfaces. In those

* Tel.: +1 801 581 5396; fax: +1 801 581 4816.
E-mail address: anil.virkar@m.cc.utah.edu.

0378-7753/$ – see front matter © 2005 Elsevier B.V. All rights reserved.
doi:10.1016/j.jpowsour.2005.01.038

Nomenclature

B_i	mobility of species i
C_i	concentration of species i
e	electronic charge
E, E_0	Nernst voltage
E_A	applied voltage
E_M	measured voltage
F	Faraday constant
g_e	electronic specific conductance
g_i	ionic specific conductance
j_i	flux of species i
I_e	electronic current density
I_i	current density due to species i (also ionic current density)
I_L	load current (density)
k_B	Boltzmann constant
ℓ	membrane thickness
n_{O_2}	number of moles of O_2 gas
p_{O_2}	partial pressure of molecular oxygen
r_e	electronic area specific resistance
r_i	ionic area specific resistance
R	ideal gas constant
R_e	electronic area specific resistance of the membrane including interfaces
R_i	ionic area specific resistance of the membrane including interfaces
R_L	load
t	time
t_i	ionic transference number
T	temperature
V_{pore}	volume of pore
z_i	valence of species i

Greek letters

δ	interface thickness
η	overpotential
μ_i	chemical potential of species i
$\tilde{\mu}_e$	electrochemical potential of electrons
$\tilde{\mu}_i$	electrochemical potential of species i
μ_{O_2}	chemical potential of oxygen gas
$\tilde{\mu}_{O^{2-}}$	electrochemical potential of oxygen ions
$\mu_{O_2}^{decomp}$	decomposition oxygen chemical potential of the membrane
$\mu_{O_2}^{membrane}$	chemical potential of oxygen in the membrane
$\mu_{O_2}^{I}$	chemical potential of oxygen in the gas phase close to the electrode I/membrane interface
$\mu_{O_2}^{II}$	chemical potential of oxygen in the gas phase close to the electrode II/membrane interface
ρ_e	electronic resistivity
ρ_i	ionic resistivity
σ_e	electronic conductivity
σ_i	conductivity due to species i (also ionic conductivity)
φ	reduced (negative) electrochemical potential of electrons
φ^{I}	reduced (negative) electrochemical potential of electrons outside the membrane close to the electrode I/membrane interface
φ^{II}	reduced (negative) electrochemical potential of electrons outside the membrane close to the electrode II/membrane interface
Φ	electrostatic potential (Galvani)

studies which have examined transport through membranes taking into account interfaces, the focus has been on either ion transport across interfaces or electron transport across interfaces, but usually not both. Phenomenological transport equations for the flux of a charged species are usually written in terms of the gradient in electrochemical potential of the species involved and the relevant transport parameters. A fundamental assumption made, albeit often tacitly, is that of the existence of local equilibrium, which leads to relations between electrochemical potentials of charged species and chemical potentials of neutral species [2,3]. For example, for the case of oxygen ions and neutral oxygen molecules (or atoms), local equilibrium may be described in terms of oxygen molecules (or atoms), electrons and oxygen ions as the species participating in the reaction.

The above general framework is assumed regardless of the prevailing point defects, vacancies or interstitials or both. Additional equations can be written in terms of the concentrations and transport properties of point defects. This, however, often requires one to make simplifying assumptions concerning the thermodynamics of defects. The assumption of local equilibrium is universally made, either explicitly or implicitly [12]. The assumption of local equilibrium in a system also implies the existence of equilibrium at any position in the system, wherein the system may be single phase or may consist of multiple phases—including the gas phase. Transport of a species occurs from one position to another (adjacent) position in response to difference (gradient) in the relevant thermodynamic potential. In MIEC materials, the transport of both ions and electronic defects is taken into account, as the conductivities of the two species are nonzero finite, and often comparable. However, when dealing with materials that are predominantly ionic conductors with negligible electronic conductivity, often it has been the practice to ignore the electronic transport altogether [13]. This may be satisfactory if the interest is only in the net current flowing through the material. The neglect of electronic current, however, amounts to an inconsistency insofar as the assumption of local equilibrium is concerned. That is, the assumption of local equilibrium and the simultaneous neglect of electronic conduction are contradictory assumptions. If lo-

cal equilibrium is assumed, which is almost always necessary for writing down relevant transport equations, the electronic conductivity cannot be assumed to be identically equal to zero. In many cases, this inconsistency often does not lead to significant problems. However, as will be discussed in this manuscript, and has been discussed to some extent in earlier manuscripts, there are many situations in which the neglect of electronic current, however small, leads to substantial difficulties in analysis—and thus also in the interpretation of experimental results [14–16].

In devices such as fuel cells and MIEC oxygen separation membranes, no external voltage is applied. Whatever voltage is developed across the membrane is the result of differences in chemical potentials of neutral species imposed and the transport properties of the membrane. However, when dealing with devices such as oxygen separation membranes under an externally applied voltage, the system then has an additional (experimental) degree of freedom, which has important consequences concerning the design of experiments and the interpretation of data, especially concerning studies on electrode kinetics or in oxygen separation under an applied voltage or water electrolysis. In devices such as solid oxide fuel cells, it is generally not possible to obtain an accurate measurement of electrode overpotential, since it is necessary to place a reference electrode on the surface—unlike in aqueous electrochemistry wherein it can be immersed in the liquid electrolyte. In order to circumvent this problem, often the so-called three-electrode system is used, wherein the electrolyte is in the form of a thick pellet. The working electrode, the counter electrode, and the reference electrode are placed in an axisymmetric arrangement. Then, to investigate electrode kinetics at the working electrode, which may be a prospective cathode for a fuel cell, an external voltage is applied across the counter and the working electrodes. An assumption is made that the externally applied voltage is essentially equivalent to that generated by the application of an external chemical potential difference, and all that is required is to measure the current (density) as a function of overpotential, the latter measured with respect to the reference electrode—and corrected for ohmic losses. This approach is assumed to represent the situation at a real cathode in a fuel cell. As will be demonstrated in this manuscript, the three-electrode system is fundamentally and physically different from a fuel cell and its use under an externally applied voltage to investigate electrode kinetics can lead to substantial error—where the magnitude of the error depends upon a number of parameters, including the magnitude of the applied voltage.

This manuscript first develops transport equations using the standard phenomenological approach. The difference compared to much of the prior work, however, is the inclusion of the electronic current in a predominantly ionic conductor—and especially its role in the estimation of the local chemical potential of oxygen, μ_{O_2}, which determines the stability of the material, and also the net current flowing through the system. This also implies the inclusion of both ionic and electronic currents through the membrane and across the electrode/membrane interfaces. Three cases of practical interest are examined: (1) oxygen separation using an MIEC membrane, (2) a fuel cell, and (3) oxygen separation under the application of an external voltage. The implications of the latter are examined for the often-used three-electrode system under an applied voltage for the investigation of electrode kinetics. All equations are developed for the case where the transport properties of a given region are constant, independent of position and μ_{O_2}. Although in many materials the transport properties are μ_{O_2}-dependent—and thus are functions of position—such a simplifying assumption is deemed necessary to allow for the development of simple analytical equations. This approach also allows for description in terms of simple equivalent circuits. If quantitative relations between transport parameters and μ_{O_2} are known, which is rarely the case for most materials (and interfacial regions), it would be a straightforward matter to numerically solve the relevant transport equations.

2. Theoretical analysis

In what follows, transport only under isothermal conditions is addressed. It is also assumed that gas transport through the porous electrodes to the electrode/membrane interfaces is sufficiently fast such that concentration polarization is negligible.[1] General transport equation for a one-dimensional flux is given by [2]:

$$j_i = -C_i B_i \nabla \tilde{\mu}_i = -C_i B_i \frac{\mathrm{d}\tilde{\mu}_i}{\mathrm{d}x} \tag{1}$$

(assuming the flux of a charged species occurs down its electrochemical potential gradient) in # ($\mathrm{cm}^{-2}\,\mathrm{s}^{-1}$), where C_i and B_i are, respectively, concentration and mobility of species i, and the electrochemical potential of species i is given by

$$\tilde{\mu}_i = \mu_i + z_i e \Phi \tag{2}$$

where μ_i is the chemical potential of species i (J or ergs), z_i the valence of species i, e the electronic charge (C), and Φ the local electrostatic potential or Galvani potential (V).

The current density due to species i for a one-dimensional case is given by

$$I_i = z_i e j_i = -\frac{\sigma_i}{z_i e} \nabla \tilde{\mu}_i = -\frac{\sigma_i}{z_i e} \frac{\mathrm{d}\tilde{\mu}_i}{\mathrm{d}x} \tag{3}$$

in $\mathrm{A\,cm}^{-2}$, where $\sigma_i = z_i^2 e^2 C_i B_i$ is the conductivity due to species i ($\mathrm{S\,cm}^{-1}$) $= 1/\rho_i$, where ρ_i is the resistivity (Ω cm). In the above, μ_i and $\tilde{\mu}_i$ are defined on a per species (per ion, per electron, per atom, or per molecule) basis. If defined on

[1] In practice, this assumption often may not be valid. For example, this assumption may not be valid when using the three-electrode system under an externally applied voltage, the implications of which are discussed later. Also, this assumption is almost certainly not valid in devices such as solid oxide fuel cells, which use porous electrodes several microns in thickness.

a per mole basis, e is replaced by the Faraday constant, F (C mol^{-1}).

Local equilibrium is assumed to prevail everywhere in the system [12]. The cation sublattice is assumed to be rigid in what follows. For an oxygen ion conductor, the equilibrium of interest is the following, namely:

$$\tfrac{1}{2}\mathrm{O}_2 + 2\mathrm{e}' \rightarrow \mathrm{O}^{2-} \tag{4}$$

Thus, at (local—at any position in the system) equilibrium [2,12]

$$\tfrac{1}{2}\mu_{\mathrm{O}_2} + 2\tilde{\mu}_e = \tilde{\mu}_{\mathrm{O}^{2-}} \tag{5}$$

where

$$\tilde{\mu}_{\mathrm{O}^{2-}} = \mu_{\mathrm{O}^{2-}} - 2e\Phi \tag{6a}$$

and

$$\tilde{\mu}_e = \mu_e - e\Phi \tag{6b}$$

Local equilibrium also implies that any changes made in chemical or electrochemical potentials (at any given position) must satisfy the following relation:

$$\tfrac{1}{2}\delta\mu_{\mathrm{O}_2} + 2\delta\tilde{\mu}_e = \delta\tilde{\mu}_{\mathrm{O}^{2-}} \tag{7}$$

where δX denotes a small deviation in the thermodynamic potential X from the equilibrium state. The above implies that the material in question must be able to transport at least two of the species (at least two of O_2 (O), O^{2-} and e), in and out, in order to maintain local equilibrium. This also implies that when potential gradients exist, one can never have the flux of any of the species (participating in the equilibrium reaction) in the above, identically equal to zero. That is, even for a predominantly ionic conductor, we must always have $I_e \neq 0$, even though it may be small. This has important implications concerning the chemical potential of oxygen and thus the very stability of the material, which will be discussed in this manuscript.

Ionic and electronic current densities are given respectively by[2]

$$I_i = I_{\mathrm{O}^{2-}} = \frac{\sigma_{\mathrm{O}^{2-}}}{2e}\nabla\tilde{\mu}_{\mathrm{O}^{2-}} = \frac{\sigma_i}{2e}\nabla\tilde{\mu}_i = \frac{\sigma_i}{2e}\frac{\mathrm{d}\tilde{\mu}_i}{\mathrm{d}x} \tag{8}$$

where i is written for O^{2-}, and

$$I_{\mathrm{e}} = \frac{\sigma_e}{e}\nabla\tilde{\mu}_e = \frac{\sigma_e}{e}\frac{\mathrm{d}\tilde{\mu}_e}{\mathrm{d}x} \tag{9}$$

Let us write

$$\varphi = -\frac{\tilde{\mu}_e}{e} = -\frac{\mu_e}{e} + \Phi \tag{10}$$

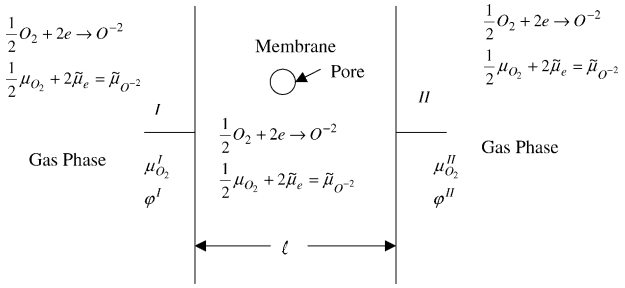

Fig. 1. A schematic illustration of a membrane of thickness ℓ, which can transport O^{2-}, e, and thus O, across which exists a difference in chemical potentials of oxygen, $(\mu^{\mathrm{I}}_{\mathrm{O}_2} - \mu^{\mathrm{II}}_{\mathrm{O}_2})$, and a difference in reduced (negative) electrochemical potentials of electrons $(\varphi^{\mathrm{I}} - \varphi^{\mathrm{II}})$. Local equilibrium in the system implies that the reaction $\frac{1}{2}\mathrm{O}_2 + 2\mathrm{e}' \rightarrow \mathrm{O}^{2-}$ is in equilibrium everywhere in the system. This means if a pore of volume V_{pore} exists at some position in the membrane, the oxygen partial pressure in the pore will be that corresponding to the local chemical potential of oxygen $\mu_{\mathrm{O}_2} = \mu^0_{\mathrm{O}_2} + RT\ln p_{\mathrm{O}_2}$, where $\mu^0_{\mathrm{O}_2}$ is the standard state chemical potential and the ideal gas law is assumed. Thus, the number of moles of O_2 in the pore is given by $n_{\mathrm{O}_2} = p_{\mathrm{O}_2}V_{\mathrm{pore}}/RT$. If now $V_{\mathrm{pore}} \rightarrow 0$, then $n_{\mathrm{O}_2} \rightarrow 0$. Yet, the local p_{O_2} (and μ_{O_2}) is well defined.

which is the Hebb notation [1]. Here φ is the (negative) reduced electrochemical potential of electrons (V). Using this notation:

$$I_e = -\sigma_e\frac{\mathrm{d}\varphi}{\mathrm{d}x} \tag{11}$$

and

$$I_i = \frac{\sigma_i}{4e}\frac{\mathrm{d}\mu_{\mathrm{O}_2}}{\mathrm{d}x} - \sigma_i\frac{\mathrm{d}\varphi}{\mathrm{d}x} \tag{12}$$

Fig. 1 shows a schematic illustration of a membrane, which can transport O^{2-}, e, and thus O (and thus also O_2), at the two electrodes of which, different chemical potentials of oxygen and different electrochemical potentials of electrons may exist. It is assumed that local equilibrium prevails at all positions in the system, including the gas phase just outside the membrane. Fig. 1 also shows the significance of local equilibrium in a fully dense material, via an example of a pore whose volume approaches zero. If a small pore exists at any position within the membrane, the local μ_{O_2} is related to the local oxygen partial pressure, p_{O_2}, by $\mu_{\mathrm{O}_2} = \mu^0_{\mathrm{O}_2} + k_{\mathrm{B}}T\ln p_{\mathrm{O}_2}$, with the number of moles of O_2 in the pore, n_{O_2}, related to p_{O_2}, the pore volume and temperature by the ideal gas law.[3] If the pore volume approaches zero, the number of moles of oxygen in the pore, n_{O_2}, approaches zero. However, the μ_{O_2} and the p_{O_2} continue to exist.Transport of ions and electrons also occurs across the two-electrode/electrolyte interfaces. The interface thicknesses are generally not known—and not well defined either. This is because interfacial regions can often be diffuse—due to compositional gradients and space charge effects. It will, nevertheless, be assumed here that the

[2] Even though in most oxygen ion conductors, transport of oxygen ions occurs by a vacancy mechanism, all transport equations are given here in a generic form—that is, without reference to a specific defect type.

[3] Or another appropriate gas law, depending upon the pressure and temperature. In this manuscript, it is assumed that the ideal gas law is applicable over the entire p_{O_2} range.

'interfacial' regions are of certain thicknesses and describe transport properties through the two interfaces in terms of the transport properties of interfacial regions of certain properties and thicknesses:

σ_i' and δ'—ionic conductivity and thickness of electrode I/membrane interface;
σ_e' and δ'—electronic conductivity and thickness of electrode I/membrane interface;
σ_i'' and δ''—ionic conductivity and thickness of electrode II/membrane interface;
σ_e'' and δ''—electronic conductivity and thickness of electrode II/membrane interface.

Thus, specific ionic conductance of interface I, namely g_i', is

$$g_i' = \frac{\sigma_i'}{\delta'} = \frac{1}{r_i'} \tag{13a}$$

in $\Omega^{-1}\,\mathrm{cm}^{-2}$ or $\mathrm{S\,cm}^{-2}$, and r_i' is the specific ionic resistance of interface I in $\Omega\,\mathrm{cm}^2$, and specific electronic conductance of interface I, namely g_e', is

$$g_e' = \frac{\sigma_e'}{\delta'} = \frac{1}{r_e'} \tag{13b}$$

in $\Omega^{-1}\,\mathrm{cm}^{-2}$ or $\mathrm{S\,cm}^{-2}$, and r_e' is the specific electronic resistance of interface I in $\Omega\,\mathrm{cm}^2$. Similarly, specific ionic and electronic conductances of interface II are given by

$$g_i'' = \frac{\sigma_i''}{\delta''} = \frac{1}{r_i''} \tag{13c}$$

and

$$g_e'' = \frac{\sigma_e''}{\delta''} = \frac{1}{r_e''} \tag{13d}$$

respectively. The preceding assumes, for simplicity, that the transport properties over the interface thickness are constant. This of course need not be the case, and general equations can be written as follows:

$$g_i' = \frac{1}{\int_0^{\delta'} \frac{\mathrm{d}x}{\sigma_i'(x)}} = \frac{1}{r_i'} \tag{14}$$

and similarly for the other specific conductances or resistances. The spatial dependence of transport properties implied in Eq. (14) is through their dependence on μ_{O_2}. In what follows, transport properties of the interfacial regions are assumed to be constant over the thickness and independent of p_{O_2}.[4] It will also be assumed that the interface thicknesses are much smaller than the membrane thickness, that is, $\delta', \delta'' \ll \ell$. It is to be noted that while it is generally not possible to separately determine conductivities and thicknesses of interface regions, the specific interface conductances (g_i', g_i'', g_e' and g_e'') or the specific interface resistances (r_i', r_i'', r_e' and r_e'') can in principle be measured experimentally.

Using the above terminology, ionic and electronic current densities across the interfaces are given by[5]

$$I_i' = -\frac{g_i'}{4e}\{\mu_{\mathrm{O}_2}^{\mathrm{I}} - \mu_{\mathrm{O}_2}'\} + g_i'\{\varphi^{\mathrm{I}} - \varphi'\} = -\frac{1}{4e}\frac{\mu_{\mathrm{O}_2}^{\mathrm{I}} - \mu_{\mathrm{O}_2}'}{r_i'} + \frac{\varphi^{\mathrm{I}} - \varphi'}{r_i'} \tag{15}$$

and

$$I_i'' = -\frac{g_i''}{4e}\{\mu_{\mathrm{O}_2}'' - \mu_{\mathrm{O}_2}^{\mathrm{II}}\} + g_i''\{\varphi'' - \varphi^{\mathrm{II}}\} = -\frac{1}{4e}\frac{\mu_{\mathrm{O}_2}'' - \mu_{\mathrm{O}_2}^{\mathrm{II}}}{r_i''} + \frac{\varphi'' - \varphi^{\mathrm{II}}}{r_i''} \tag{16}$$

as the ionic current densities across the two interfaces, and

$$I_e' = g_e'\{\varphi^{\mathrm{I}} - \varphi'\} = \frac{\varphi^{\mathrm{I}} - \varphi'}{r_e'} \tag{17}$$

and

$$I_e'' = g_e''\{\varphi'' - \varphi^{\mathrm{II}}\} = \frac{\varphi'' - \varphi^{\mathrm{II}}}{r_e''} \tag{18}$$

as the electronic current densities across the two interfaces. In the preceding equations, μ_{O_2}' and φ' are, respectively, chemical potential of oxygen and reduced (negative) electrochemical potential of electrons in the membrane, just inside electrode I/membrane interface; μ_{O_2}'' and φ'' the corresponding quantities in the membrane just inside interface II. In steady state:[6]

$$I_i' = I_i'' = I_i \tag{19}$$

and

$$I_e' = I_e'' = I_e \tag{20}$$

where I_i and I_e are, respectively, ionic and electronic current densities through the bulk of the membrane. In general, transport properties of most electrolyte or MIEC materials depend upon the local oxygen partial pressure, p_{O_2}, or chemical potential, μ_{O_2}. Thus, the relevant equations are (11) and (12), where the transport properties are μ_{O_2}-dependent, and thus position dependent. Integration of Eq. (12) gives [3]

$$\int_0^{\ell} I_i\,\mathrm{d}x = I_i\ell = \frac{1}{4e}\int_{,}^{''} \sigma_i\,\mathrm{d}\mu_{\mathrm{O}_2} - \int_{,}^{''} \sigma_i\,\mathrm{d}\varphi \tag{21}$$

[4] In general, the transport parameters of interfacial regions are functions of p_{O_2}. For example, a simple analysis based on adsorption shows that usually $r_i' \propto p_{\mathrm{O}_2}^{-1/n'}$, where n' is a positive number typically an integer. This aspect is ignored here since the objective is to provide analytical equations to describe general features. For any given material, if the dependence is known, it is a trivial matter to incorporate it and solve equations numerically.

[5] If the transport properties vary across the interfaces, then the relevant transport equations are of the form $I_i = \frac{1}{\delta'}\left\{\frac{1}{4e}\int_0^{\delta'} \sigma_i'\,\mathrm{d}\mu_{\mathrm{O}_2} - \int_0^{\delta'} \sigma_i'\,\mathrm{d}\varphi\right\}$.

[6] In three dimensions, the criterion for steady state is given by $\nabla\cdot I_i = 0$ and $\nabla\cdot I_e = 0$, where I_i and I_e are vectors.

and integration of Eq. (11) gives

$$\int_0^{\ell} I_e \, \mathrm{d}x = I_e \ell = -\int_{'}^{''} \sigma_e \, \mathrm{d}\varphi \tag{22}$$

where the integration is between the two (just inside) electrode/membrane interfaces. In what follows, ionic and electronic conductivities of the membrane will be assumed to be constant, independent of position. This allows explicit determination of fluxes in terms of transport properties, and more importantly the estimation of μ'_{O_2} and μ''_{O_2}, and φ' and φ'' in terms of measurable parameters. Also, this makes it possible to analyze a number of cases of interest analytically. The preceding equations then become

$$I_i = -\frac{\sigma_i}{4e\ell}\{\mu'_{O_2} - \mu''_{O_2}\} + \frac{\sigma_i}{\ell}\{\varphi' - \varphi''\} \tag{23}$$

and

$$I_e = \frac{\sigma_e}{\ell}\{\varphi' - \varphi''\} \tag{24}$$

The parameters, which are known (or which can in principle be determined experimentally) are the following: σ_i, σ_e, $g'_i = (1/r'_i)$, $g'_e = (1/r'_e)$, $g''_i = (1/r''_i)$, $g''_e = (1/r''_e)$, ℓ, $\mu^{\mathrm{I}}_{O_2}$, $\mu^{\mathrm{II}}_{O_2}$, φ^{I}, φ^{II}, I_i, and I_e. The unknowns are: μ'_{O_2}, μ''_{O_2}, φ', and φ''.

From the transport of electrons across interface I:

$$\varphi' = \varphi^{\mathrm{I}} - \frac{I_e}{g'_e} = \varphi^{\mathrm{I}} - r'_e I_e \tag{25}$$

From the transport of electrons across interface II:

$$\varphi'' = \varphi^{\mathrm{II}} + \frac{I_e}{g''_e} = \varphi^{\mathrm{II}} + r''_e I_e \tag{26}$$

From the transport of oxygen ions across interface I:

$$\mu'_{O_2} = \mu^{\mathrm{I}}_{O_2} + 4e\left(\frac{g'_e I_i - g'_i I_e}{g'_e g'_i}\right) = \mu^{\mathrm{I}}_{O_2} + 4e(r'_i I_i - r'_e I_e) \tag{27}$$

From the transport of oxygen ions across interface II:

$$\mu''_{O_2} = \mu^{\mathrm{II}}_{O_2} - 4e\left(\frac{g''_e I_i - g''_i I_e}{g''_e g''_i}\right) = \mu^{\mathrm{II}}_{O_2} - 4e(r''_i I_i - r''_e I_e) \tag{28}$$

Eqs. (25)–(28) describe the unknown potentials, namely, μ'_{O_2}, μ''_{O_2}, φ', and φ'', in terms of transport properties of interfaces and the net ionic and electronic current densities, namely I_i and I_e. An important point to note from Eqs. (27) and (28) is that even for a predominantly oxygen ion conducting membrane, one cannot a priori assume either r'_e or r''_e to be infinite, which makes I_e zero and the μ_{O_2} in the membrane indeterminate (product of ∞ and 0) and violates the criterion of local equilibrium.[7]. Thus, r'_e and r''_e can be very large, but not infinite. Eqs. (27) and (28) also show that usually $\mu'_{O_2} \neq \mu^{\mathrm{I}}_{O_2}$ and $\mu''_{O_2} \neq \mu^{\mathrm{II}}_{O_2}$, as this would require terms in parentheses to be identically zero—which would a very rare and a special case, and not a general case. As evident from Eqs. (27) and (28), the chemical potentials of O_2 just inside the interfaces (in the membrane) depend upon the values of r'_i, r'_e, r''_i, r''_e, I_i, and I_e.

In terms of the reduced electrochemical potentials of electrons at the two electrodes, the net electronic current density is given by

$$I_e = \frac{\varphi^{\mathrm{I}} - \varphi^{\mathrm{II}}}{\ell\rho_e + r'_e + r''_e} \tag{29}$$

and in terms of the chemical potentials of oxygen and the reduced electrochemical potentials of electrons at the two electrodes, the net ionic current density is given by

$$I_i = -\frac{1}{4e}\frac{\mu^{\mathrm{I}}_{O_2} - \mu^{\mathrm{II}}_{O_2}}{\ell\rho_i + r'_i + r''_i} + \frac{\varphi^{\mathrm{I}} - \varphi^{\mathrm{II}}}{\ell\rho_i + r'_i + r''_i} \tag{30}$$

Eqs. (29) and (30) for the electronic and ionic current densities, respectively, are given in terms of parameters which, in principle, are measurable. In what follows, the above equations are used to examine the various cases outlined earlier.

2.1. The generalized form of chemical potential of oxygen as a function of position in a membrane without the incorporation of interfaces

In what follows, let us first examine the chemical potential of oxygen as a function of position in a membrane, without the incorporation of the effect of interfaces. This approach leads to simple analytical expressions. Let us consider a membrane of thickness ℓ. The chemical potentials of oxygen at the two sides are $\mu^{\mathrm{I}}_{O_2}$ at $x = 0$ and $\mu^{\mathrm{II}}_{O_2}$ at $x = \ell$. The net electronic and ionic current densities through the membrane are given by Eqs. (11) and (12). In general, the conductivities are functions of position (which actually are functions of position-dependent chemical potential). Summing the two current densities, rearranging the terms and integrating gives:

$$\mu_{O_2}(x) = \mu^{\mathrm{I}}_{O_2} + 4e(I_i + I_e)\int_0^x \frac{\mathrm{d}x}{\sigma_i(x)} + 4e\int_{\varphi^{\mathrm{I}}}^{\varphi(x)} \left(\frac{\sigma_i(x) + \sigma_e(x)}{\sigma_i(x)}\right) \mathrm{d}\varphi(x) \tag{31}$$

The preceding shows that the chemical potential of oxygen within the membrane can be completely described by Eq. (31) provided the net current flowing through the membrane, namely $I_i + I_e$ is known, and transport properties are known as functions of position. Eq. (31) is applicable for both steady and transient states. In the transient state, all dependent variables are also time dependent, that is $\sigma_i(x, t)$, $\sigma_e(x, t)$, $\mu_{O_2}(x, t)$, $\varphi(x, t)$, $I_i(x, t)$ and $I_e(x, t)$. Yet, Kirchoff's laws are assumed applicable, which gives $I_i(x, t) + I_e(x, t) = I_{\mathrm{total}}(t)$. That is, the net current density, $I_{\mathrm{total}}(t)$, is a function of time alone. In what follows, we will only consider the steady state. In the preceding it is assumed that the chemical potentials of

[7] Obviously, r_e cannot be infinite either, as discussed in [14].

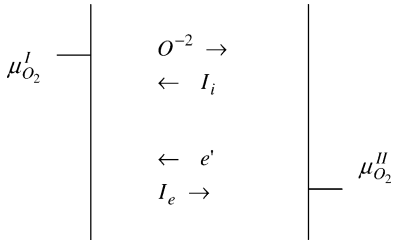

Fig. 2. A schematic illustration of an MIEC membrane under an applied difference of chemical potential of oxygen, with no applied voltage difference. Electronic and ionic currents are of equal magnitude but are in the opposite directions.

oxygen just inside the two interfaces are the same as in the local atmospheres. The exact details of the variation of $\mu_{O_2}(x)$ with position depends upon the magnitudes and spatial dependencies of the transport properties of the membrane, the end values of the chemical potentials, namely $\mu^{I}_{O_2}$ and $\mu^{II}_{O_2}$, and the end values of the reduced electrochemical potentials of electrons, namely φ^{I} and φ^{II}. If analytical relations are known between transport properties and position, Eq. (31) can be readily used to determine $\mu_{O_2}(x)$ as a function of position.[8] This is a special case wherein an assumption is made that $\mu'_{O_2} = \mu^{I}_{O_2}$ and $\mu''_{O_2} = \mu^{II}_{O_2}$. However, there is no justification for this assumption in a general case, as already stated previously. That is, in a general case, $\mu'_{O_2} \neq \mu^{I}_{O_2}$ and $\mu''_{O_2} \neq \mu^{II}_{O_2}$. Under such conditions, it is not possible to obtain a simple analytical equation (such as the one given in Eq. (31)) with transport properties dependent upon position. The objective of this work is to explore the role of interfaces and obtain explicit expressions for μ'_{O_2} and μ''_{O_2}. Hence, a simplifying assumption is made here that transport parameters are spatially invariant in the membrane. In order to account for the interfaces, as stated earlier, properties of the interfaces are separately included.

2.2. An MIEC oxygen separation membrane

In what follows, the transport properties are assumed to be independent of position within the membrane. In this case of an MIEC oxygen separation membrane, no voltage is applied across the membrane. However, a chemical potential difference of oxygen is imposed across the membrane. As there is a chemical potential difference across the membrane, a corresponding difference in electrochemical potential of electrons is created. Fig. 2 shows a schematic illustration of a MIEC membrane across which there is a gradient in the chemical potential of oxygen. Let $\mu^{I}_{O_2} > \mu^{II}_{O_2}$. Since neither an external voltage is applied, nor the membrane is externally shorted, the net current is zero. That is, $I_i + I_e = 0$ or $I_e = -I_i$.

For $\mu^{I}_{O_2} > \mu^{II}_{O_2}$, oxygen ion transport occurs from I to II (from left to right in Fig. 2). That is $I_i < 0$, and therefore, $I_e > 0$.

[8] An important point to note is that the transport properties are functions of μ_{O_2}, and their dependence on position is through the dependence of the chemical potential on position.

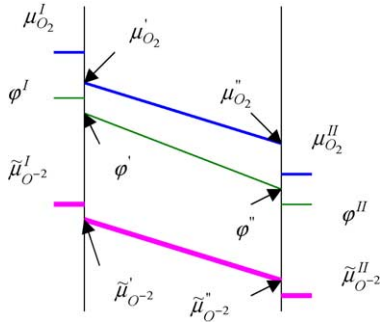

Fig. 3. Schematic variations of μ_{O_2}, $\tilde{\mu}_{O^{2-}}$ and φ for the case depicted in Fig. 2. Abrupt changes in μ_{O_2}, φ, and $\tilde{\mu}_{O^{2-}}$ are shown across interfaces since $\delta', \delta'' \ll \ell$.

The chemical potential of oxygen just below the interface at I given by Eq. (27) becomes

$$\mu'_{O_2} = \mu^{I}_{O_2} + 4e\left(\frac{g'_e + g'_i}{g'_e g'_i}\right) I_i = \mu^{I}_{O_2} - 4e\left(\frac{g'_e + g'_i}{g'_e g'_i}\right)|I_i|$$
$$= \mu^{I}_{O_2} - 4e(r'_i + r'_e)|I_i| \quad (32)$$

That is, $\mu'_{O_2} < \mu^{I}_{O_2}$.

Similarly, the reduced (negative) electrochemical potential of electrons just inside interface I is given by

$$\varphi' = \varphi^{I} - \frac{I_e}{g'_e} = \varphi^{I} + \frac{I_i}{g'_e} = \varphi^{I} - \frac{|I_i|}{g'_e} = \varphi^{I} - r'_e|I_i| \quad (33)$$

That is, $\varphi' < \varphi^{I}$.

Similar equations can be written for μ_{O_2} and φ just inside interface at II, namely μ''_{O_2} and φ''. For example note that

$$\mu''_{O_2} = \mu^{II}_{O_2} - 4e\left(\frac{g''_e + g''_i}{g''_e g''_i}\right) I_i = \mu^{II}_{O_2} + 4e\left(\frac{g''_e + g''_i}{g''_e g''_i}\right)|I_i|$$
$$= \mu^{II}_{O_2} + 4e(r''_i + r''_e)|I_i| \quad (34)$$

That is, $\mu''_{O_2} > \mu^{II}_{O_2}$.

The reduced (negative) electrochemical potential of electrons just inside interface II is similarly given by

$$\varphi'' = \varphi^{II} + \frac{|I_i|}{g''_e} = \varphi^{II} + r''_e|I_i| \quad (35)$$

That is, $\varphi'' > \varphi^{II}$.

Note also that $I_e = \frac{\sigma_e}{\ell}\{\varphi' - \varphi''\} > 0$ or $\varphi' > \varphi''$. Rearrangement of Eq. (23) gives

$$\{\mu'_{O_2} - \mu''_{O_2}\} = -\frac{4e\ell}{\sigma_i} I_i + 4e\{\varphi' - \varphi''\} \quad (36)$$

Since $I_i < 0$ and $\varphi' > \varphi''$, it is clear that $\mu'_{O_2} > \mu''_{O_2}$.

Thus, for an MIEC membrane, for the experimentally selected conditions corresponding to $\mu^{I}_{O_2} > \mu^{II}_{O_2}$, it is seen that $\mu^{I}_{O_2} > \mu'_{O_2} > \mu''_{O_2} > \mu^{II}_{O_2}$ and $\varphi^{I} > \varphi' > \varphi'' > \varphi^{II}$, regardless of the absolute values of transport parameters of the bulk membrane and interfaces. Fig. 3 shows the schematic variations of μ_{O_2} and φ for this case, where it is tacitly assumed that

$r'_e \sim r''_e \sim r_e$. Finally, as the transport of oxygen ions occurs from left to right, note that $\tilde{\mu}^{\mathrm{I}}_{\mathrm{O}^{2-}} > \tilde{\mu}'_{\mathrm{O}^{2-}} > \tilde{\mu}''_{\mathrm{O}^{2-}} > \tilde{\mu}^{\mathrm{II}}_{\mathrm{O}^{2-}}$. The spatial variation of $\tilde{\mu}_{\mathrm{O}^{2-}}$ is also shown in Fig. 3.

Since $\mu^{\mathrm{I}}_{\mathrm{O}_2} > \mu'_{\mathrm{O}_2} > \mu''_{\mathrm{O}_2} > \mu^{\mathrm{II}}_{\mathrm{O}_2}$, as long as $\mu^{\mathrm{II}}_{\mathrm{O}_2} > \mu^{\mathrm{decomp}}_{\mathrm{O}_2}$, where $\mu^{\mathrm{decomp}}_{\mathrm{O}_2}$ is the chemical potential of oxygen below which membrane decomposition can occur, the stability of the membrane is assured. An important point to note, however, is that the membrane may continue to be stable even if $\mu^{\mathrm{II}}_{\mathrm{O}_2} < \mu^{\mathrm{decomp}}_{\mathrm{O}_2}$, provided $\mu''_{\mathrm{O}_2} > \mu^{\mathrm{decomp}}_{\mathrm{O}_2}$. That is, interface properties are expected to have a profound effect in dictating membrane stability. The interface properties may also depend upon the atmosphere. For example, for a given $\mu^{\mathrm{II}}_{\mathrm{O}_2}$ (and thus for a given $p^{\mathrm{II}}_{\mathrm{O}_2}$), the μ''_{O_2} may be different in H_2/H_2O and CO/CO_2 atmospheres. Thus, it is possible that a given MIEC may be stable (permeate side) in one gas mixture but not in the other, even though the p_{O_2} in the two atmospheres is identical.

Substitution for $\mu'_{\mathrm{O}_2}, \mu''_{\mathrm{O}_2}, \varphi'$, and φ'' in terms of respective current densities and transport properties of the two interfaces into Eq. (23) gives

$$\varphi^{\mathrm{I}} - \varphi^{\mathrm{II}} = \frac{1}{4e}\{\mu^{\mathrm{I}}_{\mathrm{O}_2} - \mu^{\mathrm{II}}_{\mathrm{O}_2}\} + I_i\left[\frac{\ell}{\sigma_i} + \frac{g'_i + g''_i}{g'_i g''_i}\right]$$
$$= \frac{1}{4e}\{\mu^{\mathrm{I}}_{\mathrm{O}_2} - \mu^{\mathrm{II}}_{\mathrm{O}_2}\} + I_i[\ell\rho_i + r'_i + r''_i] \quad (37)$$

Also, from the equations for I_i and I_e, and noting that $I_i + I_e = 0$, using Eqs. (29) and (30) it is easy to see that

$$\varphi^{\mathrm{I}} - \varphi^{\mathrm{II}} = \frac{\ell\rho_e + r'_e + r''_e}{[\ell\rho_e + r'_e + r''_e] + [\ell\rho_i + r'_i + r''_i]} \frac{\mu^{\mathrm{I}}_{\mathrm{O}_2} - \mu^{\mathrm{II}}_{\mathrm{O}_2}}{4e} \quad (38)$$

Thus, in general

$$\varphi^{\mathrm{I}} - \varphi^{\mathrm{II}} < \frac{\mu^{\mathrm{I}}_{\mathrm{O}_2} - \mu^{\mathrm{II}}_{\mathrm{O}_2}}{4e}$$

If $[\ell\rho_e + r'_e + r''_e] \gg [\ell\rho_i + r'_i + r''_i]$, then

$$\varphi^{\mathrm{I}} - \varphi^{\mathrm{II}} \approx \frac{\mu^{\mathrm{I}}_{\mathrm{O}_2} - \mu^{\mathrm{II}}_{\mathrm{O}_2}}{4e} = E_0 \quad (39)$$

where E_0 is the Nernst potential.

Equivalent circuit. It is customary to represent an equivalent circuit for a bulk MIEC in terms of a Nernst voltage, generated by the imposed chemical potential difference, and ionic and electronic resistances [17]. However, for interfaces, the common practice has often been to use a capacitor in combination with a resistor [18]. The charged capacitor then models the voltage difference created by the chemical potential difference, and in fact a so-called chemical capacitance can be defined, which is meant to embody the relevant thermodynamics. The concept of chemical capacitance has also been used by some to model a bulk MIEC membrane. In such a case, a (chemical) capacitor is introduced between two sets of parallel ionic and electronic resistor segments. Fig. 4(a) shows a schematic illustration. In steady state, no current flows through the capacitor, while the ionic current is uniform in the ionic segments, and the electronic current is uniform in the electronic segments. In a transient state, the ionic currents in the two ionic segments are different and so are the electronic currents in the two electronic segments. However, Kirchoff's laws continue to hold, that is, $\nabla\cdot(I_i + I_e) = 0$, which for a one-dimensional case reduces to $I_i + I_e =$ constant. Also, in the transient state, there is a net current flowing through the capacitor.

In this manuscript, however, internal EMF sources will be used to model bulk as well as interfacial regions. Since the chemical potential varies spatially (including across interfaces), representation of interfacial regions in terms of Nernst voltages is a natural extension of the usual practice of representing bulk regions in terms of Nernst voltages. That is, there is no particular requirement, which states that one must use capacitors to describe the interfacial regions, if an EMF source is used to describe the bulk regions.

In what follows, rationale for the choice of internal EMFs to describe both bulk and interfacial regions of an MIEC under an applied chemical potential is first described. Consider the application of a net chemical potential difference across a membrane such that the position-dependent chemical potential of oxygen given by $\mu_{\mathrm{O}_2}(x)$, is a continuous function of position, x. Thus, the chemical potential at $x + \mathrm{d}x$ is given by $\mu_{\mathrm{O}_2}(x + \mathrm{d}x) = \mu_{\mathrm{O}_2}(x) + \mathrm{d}\mu_{\mathrm{O}_2}(x)$. The corresponding Nernst voltage across the slice $\mathrm{d}x$ is given by $\mathrm{d}E(x) = \frac{\mathrm{d}\mu_{\mathrm{O}_2}(x)}{4e}$. The local ionic and electronic area specific resistances for the slice are $\mathrm{d}r_i(x) = \rho_i(x)\,\mathrm{d}x$ and $\mathrm{d}r_e(x) = \rho_e(x)\,\mathrm{d}x$. The corresponding equivalent circuit for the slice is shown in Fig. 4(b). Note that the electronic and the ionic segments are joined at the ends (nodes). The significance is that the existence of local equilibrium corresponding to the reaction $\frac{1}{2}\mathrm{O}_2 + 2e' \rightarrow \mathrm{O}^{2-}$ requires the transport of ionic and electronic currents to any position, which corresponds to joining of the electronic and the ionic segments at the nodes. The equivalent circuit for the entire membrane (by discretizing it in slices of thickness $\mathrm{d}x$) is shown in Fig. 4(c). Now, no charge accumulation can occur at any node. In such a case, Kirchoff's equations must be applicable, which means

$$I_i(x,t) + I_e(x,t) = I_i(x + \mathrm{d}x, t) + I_e(x + \mathrm{d}x, t) = \cdots$$
$$= I_i(x + n\,\mathrm{d}x, t) + I_e(x + n\,\mathrm{d}x, t) \quad (40)$$

where t denotes time and n the number of differential segments. Eq. (40) is applicable both under transient and steady state conditions. For this reason, the time dependence is explicitly included. Under transient conditions, ionic current entering a node may be different from that leaving the node, and similarly for the electronic current, yet consistent with the above identity.[9] In such a case, all dependent variables,

[9] The same situation exists if one uses a capacitor (Fig. 4(a)) to describe transport. In this case, the magnitude of the difference in ionic currents entering and exiting the capacitor is the same as the magnitude of the electronic currents entering and exiting the capacitor.

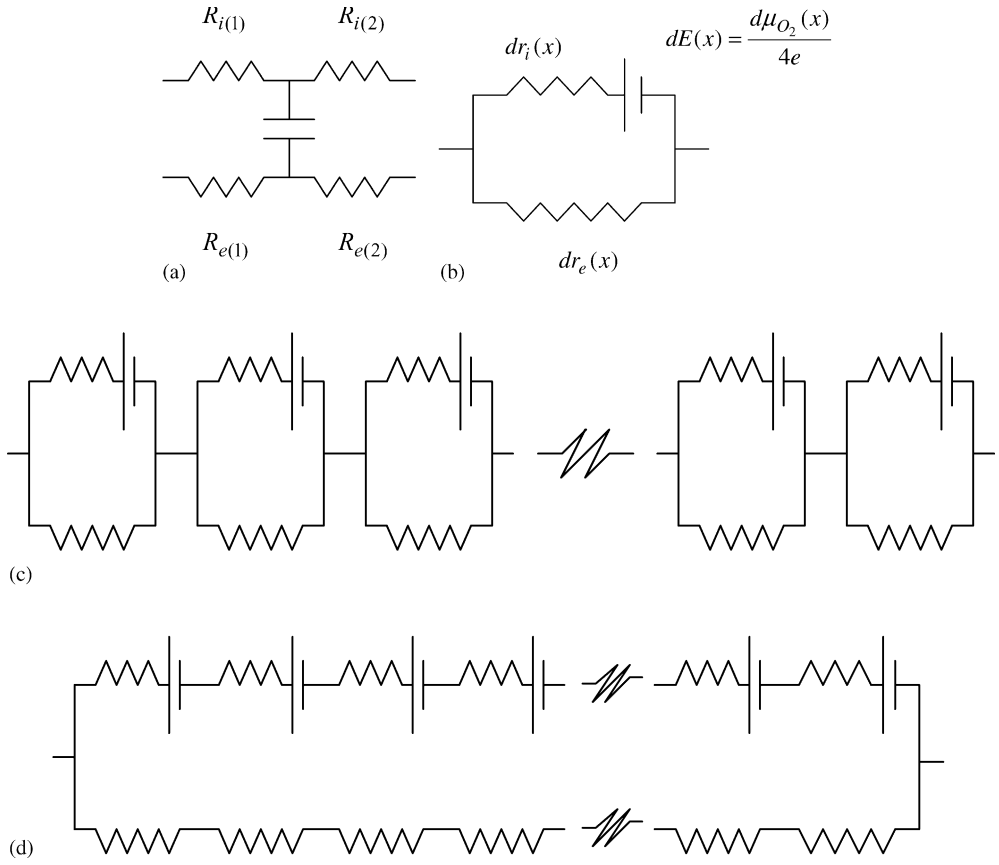

Fig. 4. (a) An equivalent circuit describing spatial variation of transport parameters through an MIEC using a chemical capacitance. (b) An equivalent circuit describing spatial variation of transport parameters through a slice dx of an MIEC using an internal EMF source, which is related to local variation in chemical potential of oxygen, d$\mu_{O_2}(x)$. (c) An equivalent circuit describing spatial variation of transport parameters through an MIEC. The equivalent circuit is applicable for both transient and steady states. For the transient state, the ionic and electronic currents are functions of position and time. However, Kirchoff's laws continue to be valid. In steady state, the ionic and electronic currents are independent of time and position (for a one-dimensional problem). (d) An equivalent circuit describing spatial variation of transport parameters through an MIEC. The equivalent circuit is applicable only for steady state.

including $\mu_{O_2}(x)$, are time dependent. Thus, in a transient state, $I_i(x,t) + I_e(x,t) = I_i(x + \mathrm{d}x, t) + I_e(x + \mathrm{d}x, t)$, however $I_i(x, t) \neq I_i(x + \mathrm{d}x, t)$ and $I_e(x, t) \neq I_e(x + \mathrm{d}x, t)$. The corresponding equivalent circuit is shown in Fig. 4(c). In such a case, the electronic and the ionic segments must be joined at the nodes. Also, in such a case, the ionic and the electronic current densities are in general time dependent.

In steady state, in addition, the divergence of ionic and electronic currents must be individually zero, that is, $\nabla \cdot I_i = 0$ and $\nabla \cdot I_e = 0$, and obviously current densities are not time dependent. For a one-dimensional case, this implies that $I_i(x) = I_i(x + \mathrm{d}x) = I_i(x + 2\,\mathrm{d}x) = \cdots = I_i(x + n\,\mathrm{d}x) = \cdots$ and $I_e(x) = I_e(x + \mathrm{d}x) = I_e(x + 2\,\mathrm{d}x) = \cdots = I_e(x + n\,\mathrm{d}x) = \cdots$. Under such conditions, the equivalent circuit may also be described by that in Fig. 4(d). Nevertheless, it is to be recognized that the general equivalent circuit applicable for both the transient and steady states is that given in Fig. 4(c). If this equivalent circuit is used for steady state, then it should be further specified that both the ionic and electronic currents satisfy the conditions $\nabla \cdot I_i = 0$ and $\nabla \cdot I_e = 0$. For a one-dimensional case, this is equivalent to ionic and electronic currents being spatially invariant. If one uses a capacitor instead, then the equivalent circuit given in Fig. 4(a) is applicable in both transient and steady states. For the steady state, no current flows through the capacitor.

The choice of μ_{O_2}-independent and position-independent properties for any given region allows for a simple equivalent circuit representation of the MIEC membrane just described. The corresponding equivalent circuit is given in Fig. 5. Note again the representation in terms of internal EMF sources rather than charged capacitors—which is consistent with the spatial variation in μ_{O_2}. The internal EMFs are given by

$$E' = \frac{\mu^{\mathrm{I}}_{O_2} - \mu'_{O_2}}{4e} = \frac{RT}{4F} \ln\left(\frac{p^{\mathrm{I}}_{O_2}}{p'_{O_2}}\right) = \frac{k_B T}{4e} \ln\left(\frac{p^{\mathrm{I}}_{O_2}}{p'_{O_2}}\right) \tag{41}$$

$$E_i = \frac{\mu'_{O_2} - \mu''_{O_2}}{4e} = \frac{RT}{4F} \ln\left(\frac{p'_{O_2}}{p''_{O_2}}\right) = \frac{k_B T}{4e} \ln\left(\frac{p'_{O_2}}{p''_{O_2}}\right) \tag{42}$$

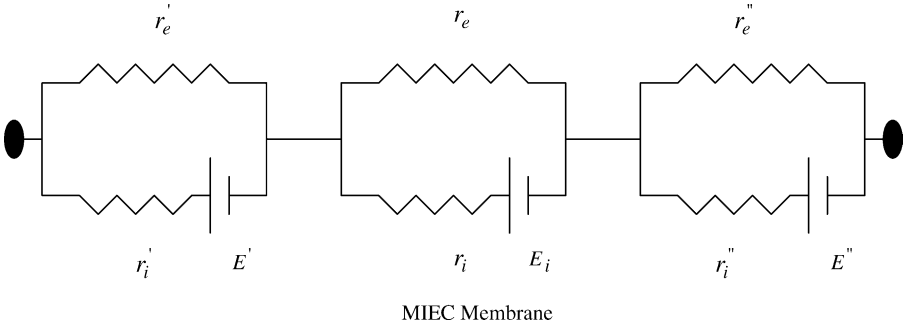

Fig. 5. An equivalent circuit for the MIEC membrane. The circuit elements between the two filled elliptical symbols are not physically separable; they collectively represent the equivalent circuit. All E's (E', E_i, E'') are of the same sign.

$$E'' = \frac{\mu''_{O_2} - \mu^{II}_{O_2}}{4e} = \frac{RT}{4F}\ln\left(\frac{p''_{O_2}}{p^{II}_{O_2}}\right) = \frac{k_B T}{4e}\ln\left(\frac{p''_{O_2}}{p^{II}_{O_2}}\right) \tag{43}$$

and their sum is given by

$$E = E' + E_i + E'' = \frac{\mu^{I}_{O_2} - \mu^{II}_{O_2}}{4e} = \frac{RT}{4F}\ln\left(\frac{p^{I}_{O_2}}{p^{II}_{O_2}}\right)$$

$$= \frac{k_B T}{4e}\ln\left(\frac{p^{I}_{O_2}}{p^{II}_{O_2}}\right) \tag{44}$$

The equivalent circuit can be readily used to solve for the currents flowing through the membrane, subject to the condition that in steady state $I'_i = I''_i = I_i$ and $I'_e = I''_e = I_e$.[10] And, also in this case of an MIEC membrane, $I_i + I_e = 0$. Let us write

$$R_i = r'_i + \ell\rho_i + r''_i = r'_i + r_i + r''_i \tag{45}$$

and

$$R_e = r'_e + \ell\rho_e + r''_e = r'_e + r_e + r''_e \tag{46}$$

where $r_i = \ell\rho_i = \ell/\sigma_i$ and $r_e = \ell\rho_e = \ell/\sigma_e$. It is easy to see that

$$I_i = -I_e = -\frac{E}{R_i + R_e} \tag{47}$$

The measured voltage across the MIEC membrane is

$$E_M = \varphi^{I} - \varphi^{II} = I_e R_e = \frac{E R_e}{R_i + R_e} \tag{48}$$

Thus, the effective ionic transference number of the membrane, including interfacial effects, is given by

$$t_i = \frac{E_M}{E} = \frac{R_e}{R_i + R_e} = \frac{r'_e + r_e + r''_e}{r'_i + r_i + r''_i + r'_e + r_e + r''_e} \tag{49}$$

Often, the measurement of open circuit voltage across an MIEC is used to estimate the transference number of the membrane material, the latter given by

$$t_i^m = \frac{r_e}{r_i + r_e} \tag{50}$$

It is clear that only in a special case when $r_e \gg r'_e + r''_e$ and $r_i + r_e \gg r'_i + r''_i + r'_e + r''_e$, will the measurement of open circuit voltage (OCV) give the material ionic transference number, t_i^m. That is, in general, the measurement of OCV cannot be used to determine the ionic or the electronic transference numbers of the material. This conclusion is similar to the one arrived at by Liu and Hu, who evaluated the effect of interfacial polarization on the apparent transference numbers of MIEC materials [19]. The effect of interfacial resistance on the apparent transference numbers in MIEC materials has also been examined by Kharton and Marques [20].

2.3. A solid oxide fuel cell

In a solid oxide fuel cell, one electrode is exposed to fuel (anode) and the other electrode is exposed to oxidant (cathode). The membrane is of a predominantly ion conducting material, usually an oxygen ion conductor. During operation, an external load is connected such that a net, finite, nonzero current flows through the membrane (and of course through the external circuit). Thus, the net current is not zero, that is $I_i + I_e \neq 0$. In what follows, electrode I is the cathode, and electrode II is the anode. During cell operation, oxygen ions transport from I to II through the membrane. It is also clear that $\mu^{I}_{O_2} > \mu^{II}_{O_2}$. Note also that $\varphi^{I} > \varphi^{II}$. Since the membrane is predominantly an ionic conductor, that is, $r_e + r'_e + r''_e \gg r_i + r'_i + r''_i$, it is clear that $|I_i| \gg |I_e|$. It is to be emphasized that, for the reasons already discussed, there must be a finite, nonzero I_e, to ensure that local equilibrium is established. Fig. 6 shows a schematic illustration.

In this case also, Eq. (37), which gives the difference between the reduced electrochemical potentials of electrons at the two electrodes in terms of the difference in chemical potentials of oxygen at the two electrodes, the ionic current density, and the net ionic resistance, is applicable. Note that there are no terms containing I_e in Eq. (37). However, it is important to note that I_e is not zero, although usually $|I_e| \ll |I_i|$ in the present case of fuel cells. Thus, the net measured current

[10] The equivalent circuit, as stated above, can also be used for analysis of the transient problem wherein $\nabla\cdot I_i \neq 0$ and $\nabla\cdot I_e \neq 0$, although $\nabla\cdot(I_i + I_e) = 0$, as discussed for one-dimensional cases in [15,16].

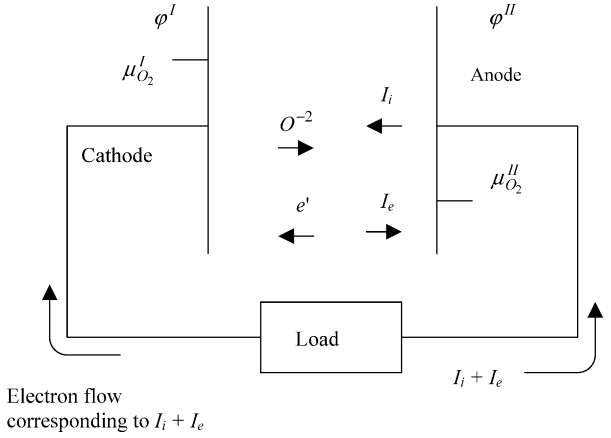

Fig. 6. A schematic illustration of a fuel cell showing the directions of oxygen ion and electron transport through the membrane. Electronic and ionic currents are in the opposite directions.

is essentially the ionic current. Also, note that $I_i < 0$. Thus, writing I as the magnitude of the measured current, note that $I_i \approx -I$. Then Eq. (37) becomes

$$\varphi^{\mathrm{I}} - \varphi^{\mathrm{II}} \approx \frac{1}{4e}\{\mu^{\mathrm{I}}_{\mathrm{O}_2} - \mu^{\mathrm{II}}_{\mathrm{O}_2}\} - I\left\{\frac{\ell}{\sigma_i} + \frac{g'_i + g''_i}{g'_i g''_i}\right\}$$
$$= \frac{1}{4e}\{\mu^{\mathrm{I}}_{\mathrm{O}_2} - \mu^{\mathrm{II}}_{\mathrm{O}_2}\} - I\{\ell\rho_i + r'_i + r''_i\} \quad (51)$$

When the fuel cell is at open circuit, the net current flowing through the external circuit, $I = 0$, which corresponds to the Nernst voltage, E_0, given by Eq. (39). This is equivalent to the establishment of (near) global equilibrium for the electrochemical potential of oxygen ions, $\tilde{\mu}_{\mathrm{O}^{2-}}$, that is $\nabla\tilde{\mu}_{\mathrm{O}^{2-}} \approx 0$. Note of course that $\nabla\tilde{\mu}_{\mathrm{O}^{2-}}$ is not identically zero, and therefore, the ionic current is not identically zero either. This situation is now equivalent to an MIEC, albeit with a very low electronic transference number, and thus $I_e = -I_i$, but with a very small magnitude. Now, consider the following seven cases corresponding to the open circuit condition: Case I: $r_e \gg r'_e, r''_e$, Case II: $r'_e \gg r_e, r''_e$, Case III: $r''_e \gg r_e, r'_e$, Case IV: $r'_e, r''_e \gg r_e$, Case V: $r_e, r''_e \gg r'_e$, Case VI: $r_e, r'_e \gg r''_e$, and Case VII: $r'_e \sim r_e \sim r''_e$. The variations of $\tilde{\mu}_{\mathrm{O}^{2-}}$, φ and μ_{O_2} for the seven cases are shown in Fig. 7. All seven cases correspond to the open circuit condition, with $[\ell\rho_e + r'_e + r''_e] \gg [\ell\rho_i + r'_i + r''_i]$, and therefore $\nabla\tilde{\mu}_{\mathrm{O}^{2-}} \approx 0$. The corresponding difference between φ^{I} and φ^{II} for all seven cases is nearly equal to the Nernst voltage, given by Eq. (39). Note, however, that the details of the variations of μ_{O_2} and φ through the interfaces and membrane depend upon the relative values of electronic resistances of the interfaces and the membrane. From the standpoint of membrane stability in a low p_{O_2} atmosphere (stability against reduction), the most preferred case is that depicted in case III, which shows that if $r''_e \gg r_e, r'_e$, the μ_{O_2} just inside the anode/electrolyte interface (that is μ''_{O_2}) will be close to the cathode side chemical potential of oxygen, namely $\mu^{\mathrm{I}}_{\mathrm{O}_2}$. This means, under such conditions, in principle, it may be possible to use an otherwise unstable electrolyte in fuel atmosphere, such as rare earth-oxide doped bismuth oxide for example, for a fuel cell application.[11] All cases considered correspond to the open circuit condition, such that $I_i + I_e = 0$. Thus, this is exactly the same as an MIEC membrane, and thus μ_{O_2} varies monotonically from the value at one electrode to the other.

When the fuel cell is shorted:

$$\varphi^{\mathrm{I}} - \varphi^{\mathrm{II}} = 0 \quad \text{or} \quad \varphi^{\mathrm{I}} = \varphi^{\mathrm{II}}$$

Thus, in this case, the electronic current density is zero, i.e., $I_e = 0$. The corresponding short circuit current density, which is exclusively due to ionic transport through the membrane, is given by

$$I_s = \frac{\mu^{\mathrm{II}}_{\mathrm{O}_2} - \mu^{\mathrm{I}}_{\mathrm{O}_2}}{4e\left\{\frac{\ell}{\sigma_i} + \frac{g'_i + g''_i}{g'_i g''_i}\right\}} = \frac{\mu^{\mathrm{II}}_{\mathrm{O}_2} - \mu^{\mathrm{I}}_{\mathrm{O}_2}}{4e\{\ell\rho_i + r'_i + r''_i\}} \quad (52)$$

Since $I_i < 0$, it is clear from Eqs. (27) and (28) that in this case also the μ_{O_2} varies monotonically. The corresponding variations of $\tilde{\mu}_{\mathrm{O}^{2-}}$, φ and μ_{O_2} for the case corresponding to $r'_e \sim r''_e \sim r_e$ are shown in Fig. 8. Various cases can be readily examined for different relative values of electronic specific resistances, similar to Fig. 7. It can be readily shown that for a given overall performance (voltage versus current density), the spatial variations of μ_{O_2} and φ can vary over a wide range, depending upon the relative values of electronic resistances.

Now let us examine the spatial variations of μ_{O_2} and φ across a fuel cell membrane when the fuel cell is under load. The chemical potentials of oxygen just inside the interfaces are given earlier. Note that $I_i < 0$ but $I_e > 0$. Thus, the term $(r'_i I_i - r'_e I_e)$ can be replaced by $-(r'_i|I_i| + r'_e|I_e|)$. An important point is that even when $|I_e| \ll |I_i|$, it is possible for $r'_i|I_i|$ and $r'_e|I_e|$ to be of comparable magnitudes, provided $r'_e \gg r'_i$. That is, the contribution of I_e for the estimation of μ_{O_2} cannot be a priori ignored. Thus, the chemical potentials of oxygen just under the interfaces are given by

$$\mu'_{\mathrm{O}_2} = \mu^{\mathrm{I}}_{\mathrm{O}_2} - 4e\left(\frac{g'_e|I_i| + g'_i|I_e|}{g'_e g'_i}\right)$$
$$= \mu^{\mathrm{I}}_{\mathrm{O}_2} - 4e(r'_i|I_i| + r'_e|I_e|) < \mu^{\mathrm{I}}_{\mathrm{O}_2} \quad (53)$$

and

$$\mu''_{\mathrm{O}_2} = \mu^{\mathrm{II}}_{\mathrm{O}_2} + 4e\left(\frac{g''_e|I_i| + g''_i|I_e|}{g''_e g''_i}\right)$$
$$= \mu^{\mathrm{II}}_{\mathrm{O}_2} + 4e(r''_i|I_i| + r''_e|I_e|) > \mu^{\mathrm{II}}_{\mathrm{O}_2} \quad (54)$$

and that the contribution of I_e to the chemical potential of oxygen cannot be a priori ignored. Thus, it is clear that $\mu^{\mathrm{I}}_{\mathrm{O}_2} > \mu'_{\mathrm{O}_2} > \mu''_{\mathrm{O}_2} > \mu^{\mathrm{II}}_{\mathrm{O}_2}$. That is, for all cases (open circuit, short circuit, and under load) of a fuel cell, the μ_{O_2} varies monotonically between the two end values. Also, therefore, as long as $\mu^{\mathrm{II}}_{\mathrm{O}_2}$ (or more accurately μ''_{O_2}) is greater than the decomposition chemical potential of the solid electrolyte,

[11] There are several difficulties, however, which may make this impractical.

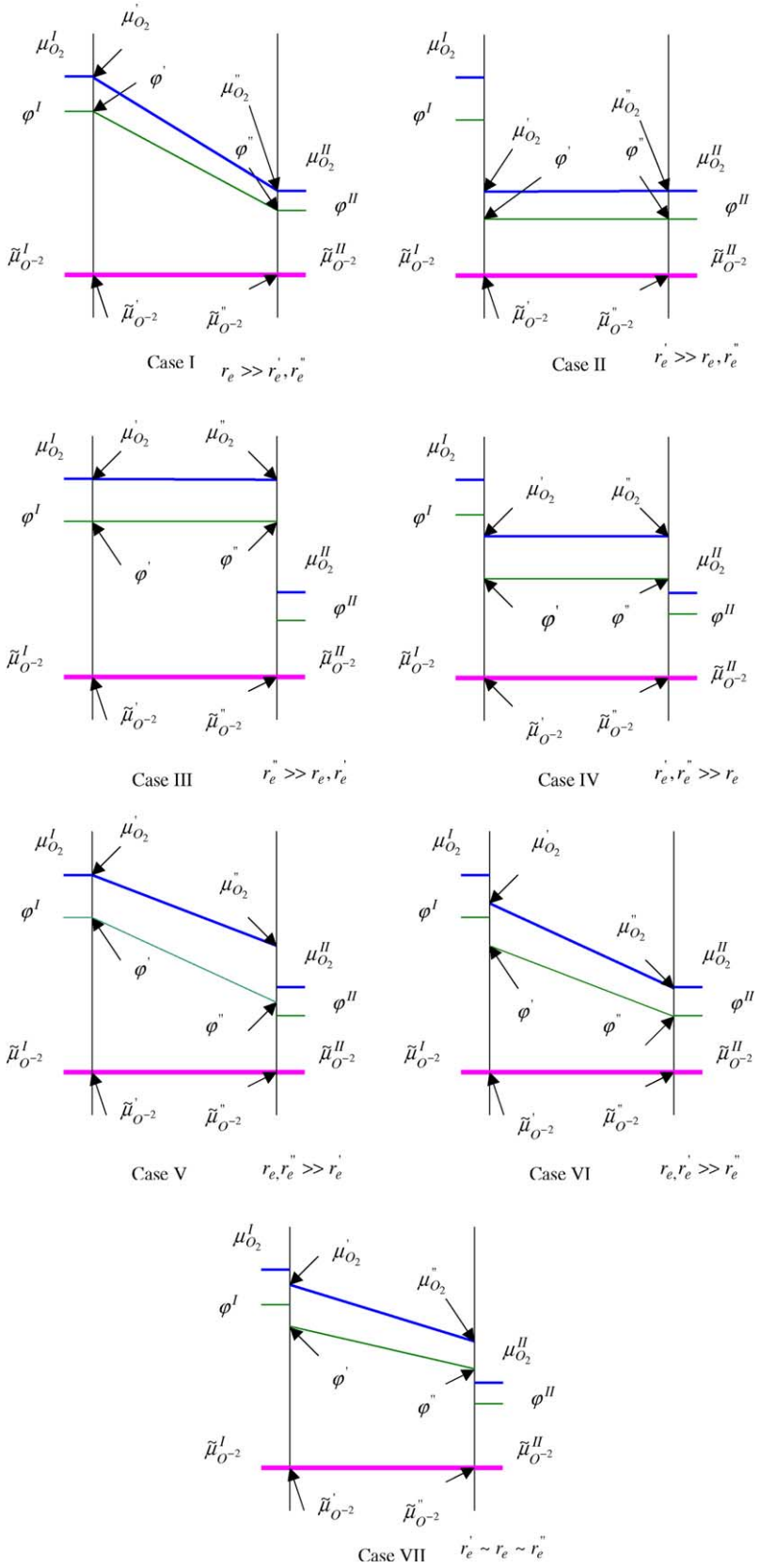

Fig. 7. Schematic variations of $\tilde{\mu}_{O^{2-}}$, φ and μ_{O_2} for different values of electronic specific resistances at open circuit through a fuel cell. Case I: $r_e \gg r_e', r_e''$, Case II: $r_e' \gg r_e, r_e''$, Case III: $r_e'' \gg r_e, r_e'$, Case IV: $r_e', r_e'' \gg r_e$, Case V: $r_e, r_e'' \gg r_e'$, Case VI: $r_e, r_e' \gg r_e''$, and Case VII: $r_e' \sim r_e \sim r_e''$. For all seven cases shown above, $R_e >> R_i$, and $\Delta\mu_{O_2} = \mu_{O_2}^{I} - \mu_{O_2}^{II} =$ fixed, which leads to $\Delta\varphi = \varphi^{I} - \varphi^{II} \approx$ fixed, and $\nabla\tilde{\mu}_{O^{2-}} \approx 0$ (near global equilibrium for O^{2-}).

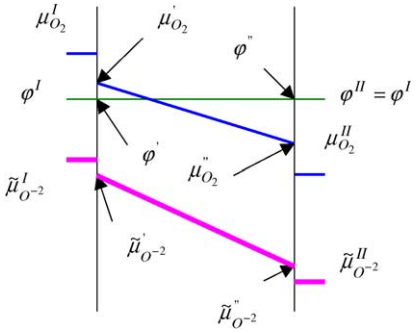

Fig. 8. Schematic variations of $\tilde{\mu}_{O^{2-}}$, φ and μ_{O_2} for a shorted cell. Note that for a shorted cell, $\Delta\varphi = \varphi^{I} - \varphi^{II} = 0$, and the electronic current through the cell is zero.

$\mu_{O_2}^{\text{decomp}}$, decomposition of the electrolyte cannot occur. It is also clear that $\varphi^{I} > \varphi' > \varphi'' > \varphi^{II}$. Schematic variations of the chemical potential of oxygen, the reduced electrochemical potential of electrons, and the electrochemical potential of oxygen ions for a fuel cell under load are shown in Fig. 9 for the case corresponding to $r_e' \sim r_e'' \sim r_e$. Note that this is qualitatively similar to that for the case of MIEC oxygen separation membrane shown in Fig. 3. Similar cases can be considered for other values of electronic area specific resistances.

Similar to the discussion on MIEC oxygen separation membranes, the corresponding equivalent circuit for a fuel cell is given in Fig. 10, with once again the provision that in steady state one must have $I_i = I_i' = I_i''$ and $I_e = I_e' = I_e''$. The equivalent circuit is similar to that for the MIEC membrane, with the exception that there is now an external load, whose resistance is given by R_L (in $\Omega\,\text{cm}^2$). The internal EMFs, and their relation to the net oxygen chemical potential difference are the same as for the MIEC membrane. However, the currents are different, by virtue of the presence of an external load. It is easy to show that

$$I_i = -\frac{E(R_e + R_L)}{R_L R_e + R_i(R_e + R_L)} \tag{55}$$

$$I_e = \frac{E R_L}{R_L R_e + R_i(R_e + R_L)} \tag{56}$$

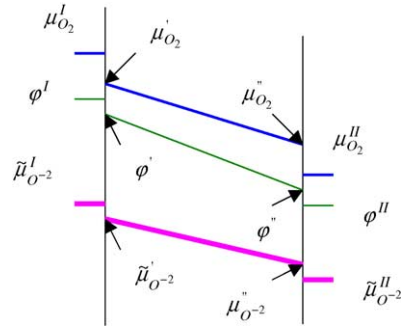

Fig. 9. Schematic variations of $\tilde{\mu}_{O^{2-}}$, φ and μ_{O_2} across a fuel cell under load.

and

$$I_L = -\frac{E R_e}{R_L R_e + R_i(R_e + R_L)} \tag{57}$$

In the above, the units of I_i, I_e and I_L are in A cm^{-2}. Note that as $R_L \to \infty$, I_i and I_e are identical in magnitude (but opposite in sign, of course), and given by Eq. (47), which is the same as for an MIEC membrane. The load current, I_L, is given by

$$I_L = I_i + I_e \tag{58}$$

The overpotentials. For a fuel cell operating with a finite, nonzero current flowing through the external circuit, there are losses associated with electrodes as well as the ohmic loss through the cell. When no load is connected, some loss continues to occur due to internal electronic leakage.[12] The rate of external work done or power is given by $I_L^2 R_L = V I_L$ where V is the voltage across the load. The rates of losses through the electrodes and through the electrolyte can be similarly calculated.

For example, for electrode I (cathode), the rate of loss (degradation of potential work into heat—an irreversible process) is given by

$$I_i^2 r_i' + I_e^2 r_e' \tag{59}$$

If r_i' and r_e' are not constant, but depend upon the local chemical potential of oxygen, then this aspect will have to be included in the analysis. For the purposes of the present discussion, r_i' and r_e' are assumed to be constant. The usual approach is to define overpotential at an electrode as a measure of the loss of useful voltage into irreversible processes. The implication is clearly that the product of the *measured* overpotential and the *measured* current (which naturally is through the external circuit) is the rate of loss of potential work into an irreversible process (heat generation). Since the measurement of current, namely I_L, is a straight forward matter, we will define overpotential at electrode I by η' such that

$$\eta' I_L = I_i^2 r_i' + I_e^2 r_e' \tag{60}$$

Thus:

$$\eta' = \frac{I_i^2 r_i' + I_e^2 r_e'}{I_L} = \frac{I_i^2 r_i' + I_e^2 r_e'}{I_i + I_e} \tag{61}$$

In the above, the overpotential at electrode I, η', is *defined* (not necessarily measurable) in terms of the rate of loss of potential useful work and the *measured* current in the external circuit, I_L. Since the rate of loss of potential work must be equal to or greater than zero (a measure of the degree of irreversibility), the product $\eta' I_L$ must be positive. In terms of the measurable parameters, the ionic and the electronic

[12] In a typical fuel cell with negligible electronic leakage, this loss is negligible, yet cannot be identically zero. However, if the electrolyte is based on ceria, internal electronic leakage can be significant.

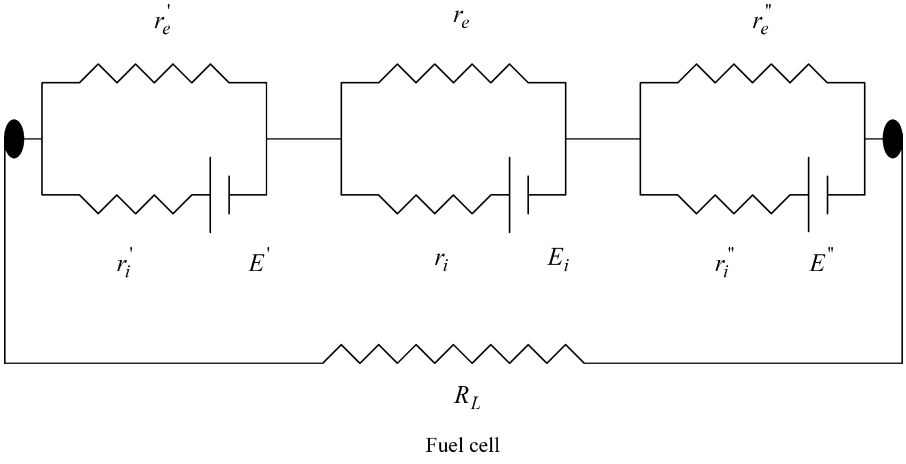

Fig. 10. An equivalent circuit for a fuel cell under an external load. The circuit elements between the two filled elliptical symbols are not physically separable; they collectively represent the equivalent circuit. All E's (E', E_i, E'') are of the same sign.

currents are given, respectively, by

$$I_i = -\frac{E}{R_i + R_e} + \frac{I_L R_e}{R_i + R_e} \tag{62}$$

and

$$I_e = \frac{E}{R_i + R_e} + \frac{I_L R_i}{R_i + R_e} \tag{63}$$

Note that as $I_L \to 0$ (open circuit), $I_e = -I_i$. Substitution for I_i and I_e, respectively, from (62) and (63) into (61) and rearrangement gives

$$\eta' = \frac{(R_e^2 r_i' + R_i^2 r_e')I_L}{(R_i + R_e)^2} + \frac{2E(R_i r_e' - R_e r_i')}{(R_i + R_e)^2} + \frac{E^2(r_i' + r_e')}{I_L(R_i + R_e)^2} \tag{64}$$

As-defined, the parameters, which can be measured, at least in principle, are the ionic and the electronic area specific resistances of the electrolyte and interfacial regions, and the current flowing through the external circuit, I_L, while η' is calculated using Eq. (64). Interesting conclusions emerge from Eq. (64). Consider first the short circuit limit. For this case, $I_e = 0$[13] and $I_i = -\frac{E}{R_i}$. Substitution into Eq. (60) or (64) and simplification gives $\eta'(\text{short circuit}) = -\frac{E}{R_i} r_i'$. This is simply the net current flowing through the external circuit multiplied by the ionic charge transfer resistance of electrode I.

Now consider the open circuit case. Under open circuit condition, no net current flows through the external circuit, that is $I_L = 0$. As no current flows through the external circuit, the obvious expectation is that the overpotential is zero. However, as discussed in what follows, this conclusion is erroneous. This is because, as long as the electronic conductivity is not identically zero, it means, $I_e = -I_i \neq 0$. Thus, at open circuit condition, according to the definition of η' given in Eqs. (60), (61) and (64), $\eta' \to -\infty$ or $|\eta'| \to \infty$. This looks like a strange conclusion. An important point to note, however, is that the relevant physical quantity is *not* the overpotential, η'. The relevant physical quantity is $\eta' I_L$; which is the rate of loss of potential useful work as heat (an irreversible process) through electrode I (cathode). Note that while $\eta' \to -\infty$ or $|\eta'| \to \infty$ as $I_L \to 0$, the product $\eta' I_L \to \frac{E^2(r_i' + r_e')}{(R_e + R_i)^2}$—is a finite positive limit—as $I_L \to 0$. But this is simply the rate of loss of potential work as heat through electrode I due to internal leakage. This is the significance of overpotential at open circuit.

An examination of Eq. (64) shows that the dependence of η' on I_L is nonlinear. This is despite the fact that all processes are assumed to be describable by various resistances.[14] The limit of Eq. (64) as $R_e \to \infty$ gives[15]

$$\eta' = I_L r_i' \tag{65}$$

which is the usual result. But this is valid only if the electronic resistance is infinite (very large compared to the ionic resistance). Also, only in this case the η' is the same as the experimentally measured overpotential.

The preceding suggests that a plot of I_L versus η'[16] should strictly not go through (0, 0) coordinates. Eq. (64) shows that there should be a minimum in $|\eta'|$. This minimum occurs at

[13] That is, the electronic current is identically equal zero. This, however, does not imply that local equilibrium is violated. The reason the electronic current is zero in this case is because the electrodes are shorted. In such a case, even though I_e through the membrane is zero, that through the combined system comprising the membrane and the external short is not zero. Also, the preceding is only for steady state. If the steady state has not been established, the position and time-dependent electronic current, $I_e(x, t)$, through the membrane need not be zero, even when externally shorted.

[14] Note, however, that the relationship between voltage across the cell and the measured current is still linear and is given by $V = \frac{E R_e}{(R_i + R_e)} - \left(\frac{R_i R_e}{R_i + R_e}\right)|I_L|$. If $R_e \to \infty$, this reduces to the usual equation $V = E - R_i|I_L|$.

[15] Once again, to emphasize, R_e strictly cannot go to infinity since this violates the assumption of local equilibrium. The above simply implies that R_e is very large.

[16] To reemphasize, the as-defined η' is calculated, not measured.

a current density given by

$$|I_L(\min)| = E\sqrt{\frac{r_i' + r_e'}{R_e^2 r_i' + R_i^2 r_e'}} \tag{66}$$

Note that when $R_e \to \infty$, $|I_L(\min)| \to 0$. Note also that although $|\eta'|$ exhibits a minimum, the product $I_L\eta'$ monotonically increases with increasing $|I_L|$, from its lowest value at OCV to its highest value at short circuit. This means, the rate of loss of potential useful work due to irreversibility of the process associated with overpotential, monotonically increases with load current.

For electrode II (anode) and the bulk membrane, similar equations can be written. They are as follows:

For electrode II (anode):

$$\eta'' = \frac{(R_e^2 r_i'' + R_i^2 r_e'')I_L}{(R_i + R_e)^2} + \frac{2E(R_i r_e'' - R_e r_i'')}{(R_i + R_e)^2} + \frac{E^2(r_i'' + r_e'')}{I_L(R_i + R_e)^2} \tag{67}$$

In the short circuit limit

$$\eta''(\text{short circuit}) = -\frac{E}{R_i} r_i'' \tag{68}$$

and under open circuit conditions

$$\eta'' I_L \to \frac{E^2(r_i'' + r_e'')}{(R_e + R_i)^2} \quad \text{as} \quad I_L \to 0$$

The limit of Eq. (67) as $R_e \to \infty$ gives $\eta'' = I_L r_i''$.
For the bulk membrane:

$$\eta_i = \frac{(R_e^2 r_i + R_i^2 r_e)I_L}{(R_i + R_e)^2} + \frac{2E(R_i r_e - R_e r_i)}{(R_i + R_e)^2} + \frac{E^2(r_i + r_e)}{I_L(R_i + R_e)^2} \tag{69}$$

In the short circuit limit

$$\eta_i(\text{short circuit}) = -\frac{E}{R_i} r_i \tag{70}$$

and under open circuit conditions

$$\eta_i I_L \to \frac{E^2(r_i + r_e)}{(R_e + R_i)^2} \quad \text{as} \quad I_L \to 0$$

The limit of Eq. (69) as $R_e \to \infty$ gives $\eta = I_L r_i$.

The total polarization loss is the sum of the three, namely

$$\eta = \eta' + \eta_i + \eta'' \tag{71}$$

which is also given by

$$\eta = \frac{R_e R_i}{R_i + R_e} I_L + \frac{E^2}{I_L(R_i + R_e)} \tag{72}$$

Note that when $R_e \to \infty$, $\eta \to I_L R_i$. From Eq. (72), the rate of loss of potential work into heat (irreversible process) in all parts of the cell is given by

$$\eta I_L = \frac{R_e R_i}{R_i + R_e} I_L^2 + \frac{E^2}{R_i + R_e} \tag{73}$$

which for $R_e \to \infty$ reduces to $I_L^2 R_i$.

Overpotentials in terms of thermodynamic potentials. The overpotential can be expressed in terms of chemical potential of O_2, μ_{O_2}, and reduced (negative) electrochemical potential of electrons, φ, by substituting for I_i and I_e into Eq. (60), and using Eqs. (29) and (30). In general, rather complicated equations result. In what follows, only the limiting case wherein the electronic resistance is much greater than the ionic resistance will be examined, that is, the case corresponding to $R_e \to \infty$. For this case, it can be readily shown that overpotential at electrode I is given by

$$\eta' = \frac{\tilde{\mu}^{\text{II}}_{O^{2-}} - \tilde{\mu}^{\text{I}}_{O^{2-}}}{2e} \frac{r_i'}{R_i'} \tag{74}$$

given in terms of the net drop in electrochemical potential of oxygen ions across the cell, the ionic resistance of the interface at I, and the net ionic resistance, or

$$\eta' = \frac{\tilde{\mu'}_{O^{2-}} - \tilde{\mu}^{\text{I}}_{O^{2-}}}{2e} \tag{75}$$

given in terms of the drop in electrochemical potential of oxygen across electrode I. As defined, the η' is negative, and the net current, I_L, is also negative. Similar equations can be written for η'' and η_i in terms of electrochemical potentials of oxygen ions. Note, however, that Eqs. (74) and (75) are valid only if the net electronic resistance is much larger than the net ionic resistance. Also, only in such a case the measured overpotential is the same as η' defined here.

2.4. Oxygen separation under the application of an external voltage

Such would be the case with yttria-stabilized zirconia (YSZ) or rare earth oxide-doped ceria as the electrolyte, with suitable electrodes applied on the two surfaces. In the first two cases considered, namely an MIEC membrane and a fuel cell, the $\Delta\mu_{O_2}$ and $\Delta\varphi$ are related to each other. Specifically, upon the application of $\Delta\mu_{O_2}$ across the membrane, a corresponding $\Delta\varphi$ appears across the membrane. In the present case, an external voltage is applied across the two electrodes, which effectively fixes the $\Delta\varphi$ across the membrane. This provides an additional experimental degree of freedom. Fig. 11 shows a schematic illustration.

In the present situation, note that oxygen is being pumped through the membrane from left to right. Thus, $I_i < 0$. Similarly, electrons are also being pumped through the membrane from left to right. Thus, $I_e < 0$. That means, both I_i and I_e are of the same sign, unlike the previous two cases. In this case, both $\Delta\mu_{O_2}$ and $\Delta\varphi$ are experimental parameters, which can

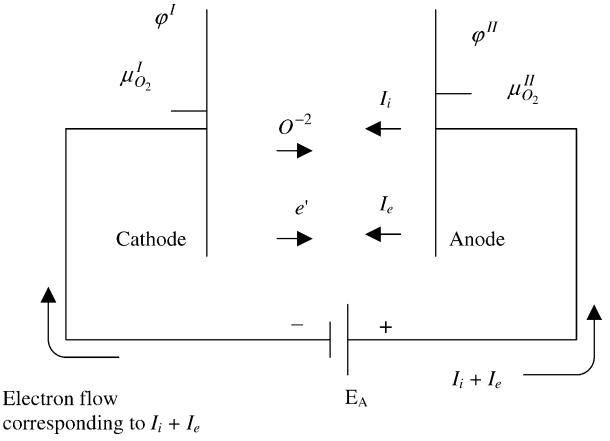

Fig. 11. A schematic illustration of an oxygen separation membrane under an externally applied voltage. Electronic and ionic currents are in the same direction.

be arbitrarily selected. The general transport equations are the same as before, and the net electronic and ionic current densities are given by Eqs. (29) and (30), respectively.

The oxygen ion current, as before, is given by Eq. (23), and the chemical potentials of oxygen just under the two interfaces are given, as before, by Eqs. (27) and (28). Since now both $I_i < 0$ and $I_e < 0$, Eqs. (27) and (28) can be written as follows:

$$\mu'_{O_2} = \mu^{I}_{O_2} + 4e\left(\frac{-g'_e|I_i| + g'_i|I_e|}{g'_e g'_i}\right)$$
$$= \mu^{I}_{O_2} - 4e(r'_i|I_i| - r'_e|I_e|) \quad (76)$$

and

$$\mu''_{O_2} = \mu^{II}_{O_2} - 4e\left(\frac{-g''_e|I_i| + g''_i|I_e|}{g''_e g''_i}\right)$$
$$= \mu^{II}_{O_2} + 4e(r''_i|I_i| - r''_e|I_e|) \quad (77)$$

Note the negative sign in parentheses. Thus, if $r'_i|I_i| > r'_e|I_e|$, note that $\mu'_{O_2} < \mu^{I}_{O_2}$, and if $r'_i|I_i| < r'_e|I_e|$, note that $\mu'_{O_2} > \mu^{I}_{O_2}$. Similarly, if $r''_i|I_i| > r''_e|I_e|$, note that $\mu''_{O_2} > \mu^{II}_{O_2}$, and if $r''_i|I_i| < r''_e|I_e|$, note that $\mu''_{O_2} < \mu^{II}_{O_2}$.

In the following discussion, it will first be assumed that $r'_i|I_i| \gg r'_e|I_e|$ and $r''_i|I_i| \gg r''_e|I_e|$. Thus, note that $\mu'_{O_2} < \mu^{I}_{O_2}$ and $\mu''_{O_2} > \mu^{II}_{O_2}$. Substitution of Eq. (30) into Eq. (76) gives

$$\mu'_{O_2} = \mu^{I}_{O_2} - \frac{\{\mu^{I}_{O_2} - \mu^{II}_{O_2}\}r'_i}{\ell\rho_i + r'_i + r''_i} + \frac{4e\{\varphi^{I} - \varphi^{II}\}r'_i}{\ell\rho_i + r'_i + r''_i} \quad (78)$$

Suppose the chemical potential of oxygen is the same at both electrodes, that is $\mu^{I}_{O_2} = \mu^{II}_{O_2}$. Then:

$$\mu'_{O_2} = \mu^{I}_{O_2} + \frac{4e\{\varphi^{I} - \varphi^{II}\}r'_i}{\ell\rho_i + r'_i + r''_i} = \mu^{I}_{O_2} - \frac{4e\{\varphi^{II} - \varphi^{I}\}r'_i}{\ell\rho_i + r'_i + r''_i} \quad (79)$$

Since $\varphi^{II} > \varphi^{I}$, note that $\mu'_{O_2} < \mu^{I}_{O_2}$. The absolute value of μ'_{O_2} in relation to $\mu^{I}_{O_2}$ depends upon the various transport parameters, especially r'_i, and the net voltage difference, namely, $\Delta\varphi = \varphi^{II} - \varphi^{I}$. The higher are the r'_i and $\Delta\varphi = \varphi^{II} - \varphi^{I}$, the lower is μ'_{O_2}. If μ'_{O_2} is lower than the decomposition potential of the electrolyte, decomposition can occur, effectively increasing the magnitude of the ionic current density, beyond that given by Eq. (23). In the case of zirconia, for example, the decomposition reaction may involve the following steps. When the $\mu'_{O_2} < \mu^{decomp}_{O_2}$, reaction:

$$ZrO_2 \rightarrow Zr^{4+} + 2O^{2-}$$

occurs just under electrode I. The oxygen ions released transport through the membrane to electrode II where the following reaction occurs:

$$2O^{2-} \rightarrow O_2(g) + 4e'$$

The electrons released transport in the external circuit to electrode I where the following reaction occurs:

$$Zr^{4+} + 4e \rightarrow Zr(\text{metal})$$

The net reaction is

$$ZrO_2 \rightarrow Zr(\text{metal, formed at negative electrode})$$
$$+ O_2(\text{g, released at positive electrode})$$

The corresponding current appears in the external circuit, in addition to the current due to oxygen pumping from left to right. An important point is that the corresponding electron transport occurs in the external circuit.

Also an important point to note is that only in a very special case would one have $\mu'_{O_2} = \mu^{I}_{O_2}$.[17] In almost all practical situations, such as the one assumed here, one would almost always have $\mu'_{O_2} < \mu^{I}_{O_2}$ (for the assumed case of $r'_i|I_i| \gg r'_e|I_e|$).

Similar analysis can be carried out for the interface at II. For the case of $\mu^{I}_{O_2} = \mu^{II}_{O_2}$, it is seen that

$$\mu''_{O_2} = \mu^{I}_{O_2} + \frac{4e\{\varphi^{II} - \varphi^{I}\}r''_i}{\ell\rho_i + r'_i + r''_i} \quad (80)$$

for the assumed case of $r''_i|I_i| \gg r''_e|I_e|$. That is, one would have

$$\mu''_{O_2} > \mu^{II}_{O_2} = \mu^{I}_{O_2}$$

Schematic variations of μ_{O_2} and φ for this special case are shown in Fig. 12. Also shown in the figure is a schematic variation of $\tilde{\mu}_{O^{2-}}$.

If, on the other hand, $r'_i|I_i| < r'_e|I_e|$ and $r''_i|I_i| < r''_e|I_e|$, we would have had $\mu'_{O_2} > \mu^{I}_{O_2}$ and $\mu''_{O_2} < \mu^{II}_{O_2}$. In such a case, the variation of μ_{O_2} and φ would be as shown schematically in Fig. 13. In such a case, the decomposition of the electrolyte can occur at the positive electrode instead. Once again the

[17] For the general case (Eq. (76)), for μ'_{O_2} to be equal to $\mu^{I}_{O_2}$, it is necessary that $r'_i|I_i| - r'_e|I_e| = 0$. Clearly, this is a very rare case, and unlikely to be realized in practice.

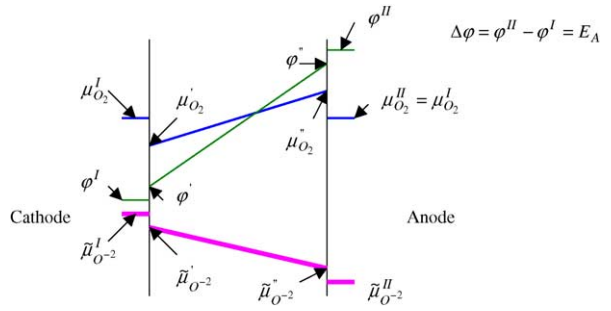

Fig. 12. Schematic variations of μ_{O_2}, φ, and $\tilde{\mu}_{O^{2-}}$ across an oxygen separation membrane under an externally applied voltage. It is assumed here that $r'_i|I_i| > r'_e|I_e|$ and $r''_i|I_i| > r''_e|I_e|$. Note that the $\tilde{\mu}_{O^{2-}}$ decreases from left to right, consistent with net oxygen transport from left to right.

reaction steps are as follows. When the $\mu''_{O_2} < \mu^{\text{decomp}}_{O_2}$, reaction

$$ZrO_2 \rightarrow Zr^{4+} + 2O^{2-}$$

occurs just under electrode II. Also at electrode II

$$2O^{2-} \rightarrow O_2(g) + 4e'$$

Electrons released transport through the external circuit to electrode I, and then through the membrane towards electrode II, where the following reaction occurs:

$$Zr^{4+} + 4e' \rightarrow Zr(\text{metal})$$

The net reaction is

$$ZrO_2 \rightarrow Zr(\text{metal, formed at positive electrode}) + O_2(g, \text{released at positive electrode})$$

In this case, however, it is necessary for the corresponding electron transport to occur through the membrane. Since the membrane is predominantly an ionic conductor, electronic conduction is expected to be negligible. The implication is that although the analysis shows that decomposition can occur at the positive electrode, the associated transport kinetics

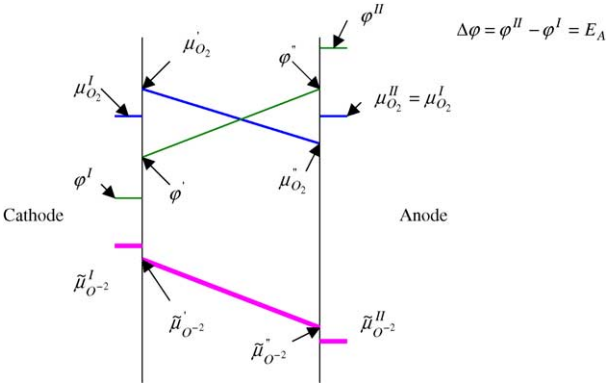

Fig. 13. Schematic variations of μ_{O_2}, φ, and $\tilde{\mu}_{O^{2-}}$ across an oxygen separation membrane under an externally applied voltage. It is assumed here that $r'_i|I_i| < r'_e|I_e|$ and $r''_i|I_i| < r''_e|I_e|$. Note that the $\tilde{\mu}_{O^{2-}}$ decreases from left to right, consistent with net oxygen transport from left to right.

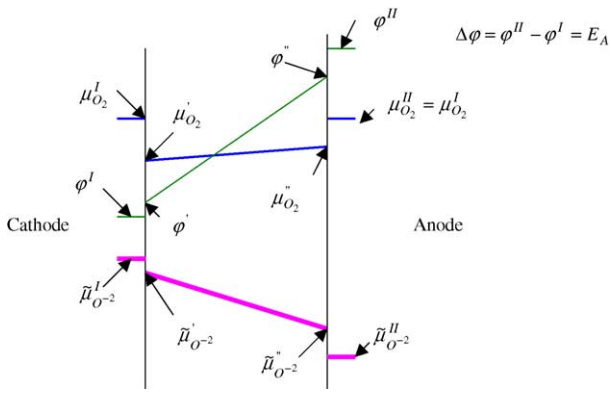

Fig. 14. Schematic variations of μ_{O_2}, φ, and $\tilde{\mu}_{O^{2-}}$ across an oxygen separation membrane under an externally applied voltage. It is assumed here that $r'_i|I_i| > r'_e|I_e|$ and $r''_i|I_i| < r''_e|I_e|$. In this case, the μ_{O_2} in the membrane everywhere is lower than that in the gas phase. Whether the μ_{O_2} increases or decreases from left to right depends upon relative magnitudes of transport parameters. Note that the $\tilde{\mu}_{O^{2-}}$ decreases from left to right, consistent with net oxygen transport from left to right.

may be very sluggish. Thus, in practice, this case may not be observed.

Additional cases can be similarly considered. They are as follows:

Suppose $r'_i|I_i| < r'_e|I_e|$, so that $\mu'_{O_2} > \mu^{I}_{O_2}$, and $r''_i|I_i| < r''_e|I_e|$, so that $\mu''_{O_2} < \mu^{II}_{O_2}$. Fig. 14 shows the expected variation of the chemical potential of oxygen through the membrane for $\mu^{II}_{O_2} = \mu^{I}_{O_2}$. Note that in this case, the μ_{O_2} in the membrane is lower than that in the gas phase.

Suppose now $r'_i|I_i| > r'_e|I_e|$, so that $\mu'_{O_2} < \mu^{I}_{O_2}$, and $r''_i|I_i| > r''_e|I_e|$, so that $\mu''_{O_2} > \mu^{II}_{O_2}$. Fig. 15 shows the expected variation of the chemical potential of oxygen through the membrane. In this case, the μ_{O_2} in the membrane is higher than that in the gas phase. The preceding shows the importance of incorporating the electronic current through

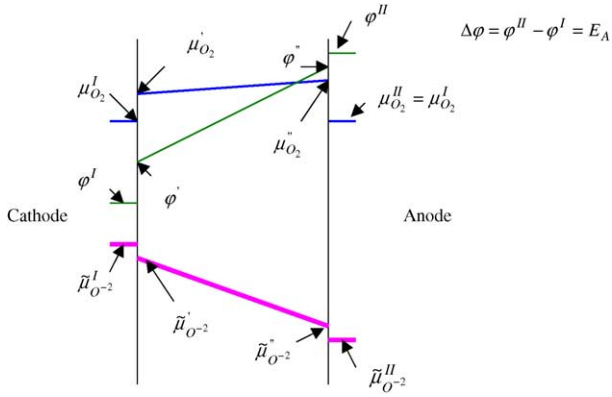

Fig. 15. Schematic variations of μ_{O_2}, φ, and $\tilde{\mu}_{O^{2-}}$ across an oxygen separation membrane under an externally applied voltage. It is assumed here that $r'_i|I_i| < r'_e|I_e|$ and $r''_i|I_i| > r''_e|I_e|$. In this case, the μ_{O_2} in the membrane everywhere is higher than that in the gas phase. Whether the μ_{O_2} increases or decreases from left to right depends upon relative magnitudes of transport parameters. Note that the $\tilde{\mu}_{O^{2-}}$ decreases from left to right, consistent with net oxygen transport from left to right.

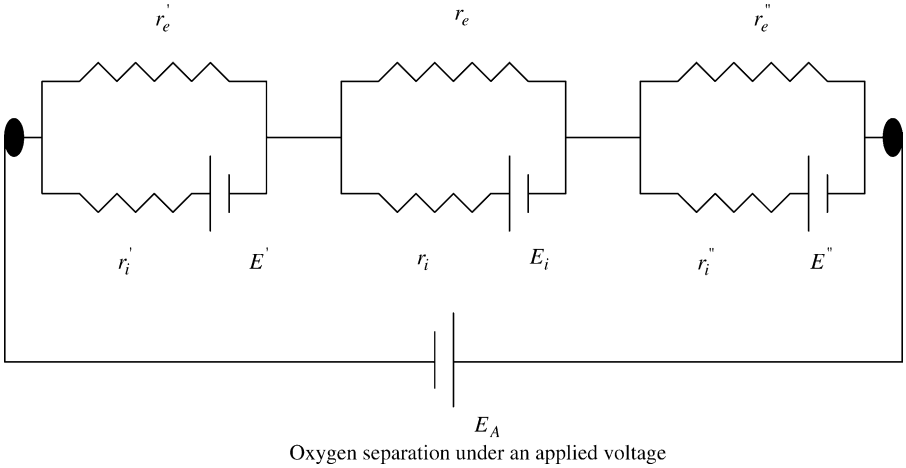

Fig. 16. An equivalent circuit for an oxygen separation membrane under an applied DC voltage. The circuit elements between the two filled elliptical symbols are not physically separable; they collectively represent the equivalent circuit. The E's (E', E_i, E'') can be of different signs, and depend upon the applied voltage, E_A, and the logarithm of the ratio of oxygen partial pressures at the two electrodes. Their sum, however, is independent E_A, but depends only on the logarithm of the ratio of oxygen pressures at the two electrodes.

bulk and also across interfaces, however small, into the transport equations, even when dealing with membranes made of predominantly oxygen ion conductors.

The equivalent circuit for an oxygen separation membrane under an externally applied voltage is given in Fig. 16 with the provision that in steady state $I_i = I_i' = I_i''$ and $I_e = I_e' = I_e''$. The same equivalent circuit is applicable for the transient case, in which the ionic and electronic currents are functions of position and time, but Kirchoff's equations continue to hold.[18] In what follows, only the steady state is considered. In this case, as before:

$$E = E' + E_i + E'' = \frac{RT}{4F}\ln\left(\frac{p'_{O_2}}{p^{I}_{O_2}}\right) + \frac{RT}{4F}\ln\left(\frac{p''_{O_2}}{p'_{O_2}}\right) + \frac{RT}{4F}\ln\left(\frac{p^{II}_{O_2}}{p''_{O_2}}\right) = \frac{RT}{4F}\ln\left(\frac{p^{II}_{O_2}}{p^{I}_{O_2}}\right) = \frac{k_B T}{4e}\ln\left(\frac{p^{II}_{O_2}}{p^{I}_{O_2}}\right) \quad (81)$$

In the previous two examples, that is an MIEC membrane and a fuel cell, all three internal EMFs were of the same sign—consistent with a monotonic variation of μ_{O_2} from one side to the other. In the present example of voltage-driven oxygen separation, however, this is not the case. Thus, the signs of the three EMFs in general are different as discussed earlier. An important point to note is that the net E in the above equation, however, is still independent of the externally applied voltage, and is only a function of $\Delta\mu_{O_2}$ existing across the membrane. However, the individual internal EMFs, namely, E', E_i, and E'' are functions of the applied voltage, E_A, and thus do determine the stability of the membrane. For the case where $\mu^{I}_{O_2} = \mu^{II}_{O_2}$, the $E = 0$. The corresponding internal EMFs at steady state are given by

$$E' = E_A\left(\frac{r'_e}{R_e} - \frac{r'_i}{R_i}\right), \qquad E_i = E_A\left(\frac{r_e}{R_e} - \frac{r_i}{R_i}\right) \quad \text{and}$$

$$E'' = E_A\left(\frac{r''_e}{R_e} - \frac{r''_i}{R_i}\right) \quad (82)$$

Note that the terms in parentheses determine the signs of the individual EMFs, yet the sum of the three EMFs is zero.

If $\mu^{I}_{O_2} \neq \mu^{II}_{O_2}$, then $E \neq 0$. Then, it can be readily shown that the various EMFs are given by

$$E' = E_A\left(\frac{r'_e}{R_e} - \frac{r'_i}{R_i}\right) + E\frac{r'_i}{R_i},$$

$$E_i = E_A\left(\frac{r_e}{R_e} - \frac{r_i}{R_i}\right) + E\frac{r_i}{R_i} \quad \text{and}$$

$$E'' = E_A\left(\frac{r''_e}{R_e} - \frac{r''_i}{R_i}\right) + E\frac{r''_i}{R_i} \quad (83)$$

and the sum of the three EMFs equals that given by Eq. (81).

The overpotentials. In the case of oxygen pumping under an applied voltage, an external agency does work on the system. Under isothermal conditions, with oxygen gas assumed to behave as an ideal gas, the internal energy is a function of temperature only. Thus, no change in the internal energy occurs upon isothermal pumping. We will first consider here the case wherein the oxygen partial pressures at the two electrodes are identical so that $\mu^{I}_{O_2} = \mu^{II}_{O_2}$ and the net E given by Eq. (81) is zero. This means all work done on the system is degraded as heat (an irreversible process). The net ionic and electronic current densities are given by $I_i = -\frac{E_A}{R_i}$ and $I_e = -\frac{E_A}{R_e}$. Then, the rate of loss of input work into heat at electrode I is given by

$$I_i^2 r'_i + I_e^2 r'_e = E_A^2\left(\frac{r'_i}{R_i^2} + \frac{r'_e}{R_e^2}\right) \quad (84)$$

[18] For membranes with spatially dependent transport properties (but without the incorporation of interfacial effects), the transient case was previously examined in [15,16].

Once again, the overpotential η' is *defined* in terms of the current measured in the external circuit, I, by

$$\eta' I = I_i^2 r_i' + I_e^2 r_e' = E_A^2 \left(\frac{r_i'}{R_i^2} + \frac{r_e'}{R_e^2} \right) \tag{85}$$

where $I = -E_A \left(\frac{1}{R_i} + \frac{1}{R_e} \right)$ and the overpotential is given by

$$\eta' = -E_A \frac{r_i' R_e^2 + r_e' R_i^2}{R_i R_e (R_i + R_e)} \tag{86}$$

In this case, as I_i and I_e are of the same sign, the η' is the same as the measured overpotential. If the electronic resistance is much larger than the ionic resistance, that is in the limit $R_e \to \infty$, the above reduces to

$$\eta' = -\frac{E_A}{R_i} r_i' = I r_i' \tag{87}$$

In terms of electrochemical potential of oxygen ions, the overpotential can be given as before by

$$\eta' = \frac{\tilde{\mu}'_{O^{2-}} - \tilde{\mu}^{I}_{O^{2-}}}{2e} \tag{88}$$

In the above, as-defined, both I and η' are negative. Similar equations can be given for η and η'', which are, respectively, overpotential losses across the bulk membrane and electrode II. It is readily shown that the net rate of degradation of input work into heat is given by $(\eta' + \eta + \eta'')I = E_A^2 \left(\frac{1}{R_i} + \frac{1}{R_e} \right)$, which for $R_e \to \infty$ reduces to $\frac{E_A^2}{R_i}$.

Suppose we now consider the case wherein $\mu^{I}_{O_2} \neq \mu^{II}_{O_2}$, such that $E = \frac{\mu^{II}_{O_2} - \mu^{I}_{O_2}}{4F} \neq 0$. In such a case, it can readily shown that the ionic and electronic currents are given by

$$I_i = -\frac{E_A - E}{R_i} \quad \text{and} \quad I_e = -\frac{E_A}{R_e} \tag{89}$$

When 1 mol of oxygen gas is pumped from $p^{I}_{O_2}$ to $p^{II}_{O_2}$, the amount of potential work degraded as heat is

$$Q = 4F(E_A - E) + \frac{4FEE_A}{E_A - E} \frac{R_i}{R_e} \tag{90}$$

and the net work of compressing 1 mol of gas from $\mu^{I}_{O_2}$ ($p^{I}_{O_2}$) to $\mu^{II}_{O_2}$ ($p^{II}_{O_2}$) is given by $w = 4FE = RT \ln \left(\frac{p^{II}_{O_2}}{p^{I}_{O_2}} \right)$. Note that if $R_e \gg R_i$ (or $R_e \to \infty$), the above reduces to $Q \approx 4F(E_A - E)$. If, however, $R_e \neq \infty$, but if $E_A = E$, then the $Q \to \infty$. Note that in this case, $I_i = 0$. Thus, it will take infinite time to transport 1 mol of oxygen. However, $I_e \neq 0$. As a result, infinite electronic charge will have to be transported in the time required to transport 1 mol of oxygen gas, which leads to $Q \to \infty$. Finally, the overpotentials can be easily determined in terms of I_i, I_e and the various area specific resistances, using the approach described earlier.

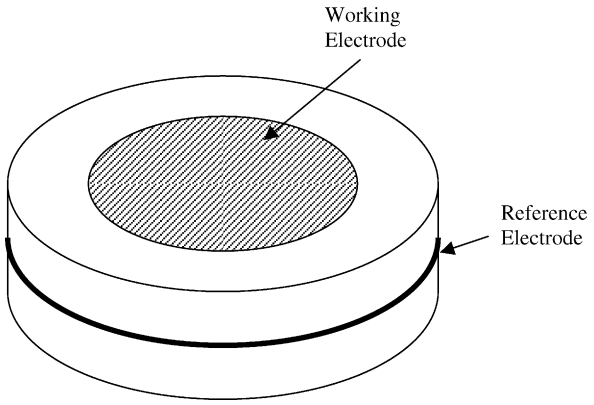

Fig. 17. A schematic illustration of the three-electrode system. A DC voltage is applied across the working electrode and the counter electrode (on the opposite face). Both current and voltage between the working and the reference electrodes are measured as a function of the applied voltage. Usually, the testing is conducted in air, although can be conducted in other environments.

2.5. The analysis of three-electrode system

Often, the placement of a reference electrode in devices such as solid oxide fuel cells (SOFC) raises questions concerning the validity of the measurement, because the reference electrode location is on the surface. In thin, electrolyte film, electrode-supported SOFC, this leads to substantial errors. In an attempt to circumvent these uncertainties, several investigators have used the three-electrode system. It consists of a thick electrolyte disc, upon which working and counter electrodes are placed on the opposite sides of the disc in a symmetric arrangement, and a reference electrode is placed in a symmetric arrangement with respect to the two electrodes. Fig. 17 shows a typical arrangement. Then, in order to investigate electrode kinetics at the working electrode, which may be a prospective cathode for SOFC, a DC voltage is applied across the working and the counter electrodes.[19] Both current through the cell and voltage across the working and reference electrodes are measured as functions of the applied voltage. Corrected for the ohmic loss, the measured voltage between the working and the reference electrodes gives a measure of the electrode overpotential at the working electrode. In what follows, implications of such measurements are described using the analysis presented so far.

The membrane or the disc is predominantly an oxygen ion conductor. Thus, note that $|I_e| \ll |I_i|$. In the following illustration, it is assumed that $r_i'|I_i| \gg r_e'|I_e|$ and $r_i''|I_i| \gg r_e''|I_e|$.[20]

[19] In many experimental procedures, the instrument is operated in such a mode so as to only track the voltage between the working and the reference electrodes, and little attention is paid to the actual voltage between the working and the counter electrodes. It is to be emphasized that from the standpoint of electrolyte stability and the present discussion, it is important to know the actual applied voltage, which is between the working and the counter electrodes. That is, the measurement of voltage between the working and reference electrodes is not sufficient to describe the problem completely.

[20] Since $|I_i| \gg |I_e|$, this also implies that $R_e \gg R_i$.

The chemical potential of oxygen just under interface I is given by Eq. (78). The testing is typically done in air. Thus, the chemical potential of oxygen at the two electrodes (just outside the electrodes) is the same. If concentration polarization is negligible, the chemical potentials of oxygen at the two electrode/electrolyte interfaces, namely $\mu^{\mathrm{I}}_{\mathrm{O}_2}$ and $\mu^{\mathrm{II}}_{\mathrm{O}_2}$ are identical, that is $\mu^{\mathrm{I}}_{\mathrm{O}_2} = \mu^{\mathrm{II}}_{\mathrm{O}_2}$. Let us consider this case first. Eq. (78) then becomes

$$\mu'_{\mathrm{O}_2} = \mu^{\mathrm{II}}_{\mathrm{O}_2} - \frac{4e\{\varphi^{\mathrm{II}} - \varphi^{\mathrm{I}}\}r'_i}{\ell\rho_i + r'_i + r''_i} \tag{91}$$

If μ'_{O_2} decreases below the decomposition chemical potential, $\mu^{\mathrm{decomp}}_{\mathrm{O}_2}$, the decomposition can occur just under electrode I, which manifests as excess current. It is also possible that a nonstoichiometry (oxygen deficiency) may develop at a lower applied voltage, which can also lead to excess current (beyond that due to the cathodic reaction, namely $\frac{1}{2}\mathrm{O}_2 + 2\mathrm{e}' \rightarrow \mathrm{O}^{2-}$). Since the experimenter has no way of determining how much of the current is due to decomposition (or nonstoichiometry development) and how much is actually attributable to the cathodic reaction occurring at electrode I, the entire current is inadvertently assigned to the cathodic reaction leading to an overestimation of cathodic activity, and thus an incorrect result. The $\mu^{\mathrm{decomp}}_{\mathrm{O}_2}$ can in principle be estimated from the known thermodynamic data. The usual assumption made during such tests is that all that needs to be done is to correct for the ohmic drop, in order to ensure that the applied voltage is less than some critical value to ensure that the chemical potential in the electrolyte is greater than $\mu^{\mathrm{decomp}}_{\mathrm{O}_2}$ [21]. For the condition $\mu'_{\mathrm{O}_2} \approx \mu^{\mathrm{decomp}}_{\mathrm{O}_2}$, Eq. (91) can be rearranged as

$$\varphi^{\mathrm{II}} - \varphi^{\mathrm{I}} \approx \left(\frac{\mu^{\mathrm{II}}_{\mathrm{O}_2} - \mu^{\mathrm{decomp}}_{\mathrm{O}_2}}{4e}\right)\left(\frac{\ell\rho_i + r'_i + r''_i}{r'_i}\right) \tag{92}$$

Eq. (92) shows that if the applied voltage exceeds the above value, decomposition of the electrolyte will occur at electrode I. The equation, however, shows that there is no way to correct for the ohmic loss as usually both r'_i and r''_i are unknowns. In the extreme case in which $r'_i \gg r''_i$ and $r'_i \gg \ell\rho_i$, Eq. (92) reduces to

$$\varphi^{\mathrm{II}} - \varphi^{\mathrm{I}} \approx \left(\frac{\mu^{\mathrm{II}}_{\mathrm{O}_2} - \mu^{\mathrm{decomp}}_{\mathrm{O}_2}}{4e}\right) \tag{93}$$

Eq. (93) gives the minimum applied voltage necessary to cause decomposition of the electrolyte for the relative values of transport parameters assumed here. Beyond this voltage, the measured current will have two components; current due to the cathodic reaction and current due to decomposition. In many cases, nonstoichiometry may appear at applied voltages lower than given by Eq. (92) or (93), and this also will contribute to excess current. In either case, the measured current will be greater than that corresponding to the cathodic reaction, leading to an overestimation of the electrode activity. That is, one may erroneously conclude that the electrocatalytic activity of the prospective cathode is far better than it really is. Fig. 18 shows a schematic illustration of the experimentally measured current (or current density) plotted versus experimentally measured overpotential in a typical three-electrode system under an applied DC bias. In the schematic illustration shown in Fig. 18, both the current and overpotential are plotted on linear scales. Hence the curvature is concave up. If the overpotential is plotted on a linear scale but the current is plotted on a logarithmic scale, the curvature will be convex up.

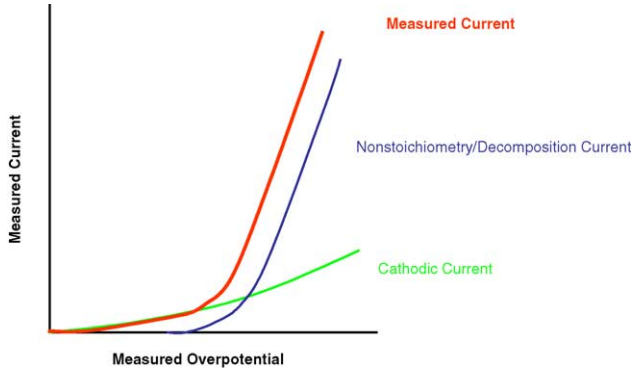

Fig. 18. A schematic illustration of the measured current (or current density) (—) vs. measured overpotential (corrected for the ohmic drop) using a three-electrode system under an applied DC voltage. It contains two parts: (a) the cathodic current (—), namely due to the reaction $\frac{1}{2}\mathrm{O}_2 + 2\mathrm{e}' \rightarrow \mathrm{O}^{2-}$, and (b) the current due to the development of nonstoichiometry or decomposition (—). In practice, it is quite possible that the nonstoichiometry/decomposition current may be much greater than the cathodic current. Under such conditions, the three-electrode system can grossly overestimate the cathodic activity. The schematic shows both current and overpotential plotted on linear scales. If the current is plotted on a logarithmic scale, the curves will be convex up.

In the preceding discussion, it was assumed that concentration polarization is negligible. In practice, if the electrode thickness is large and/or electrode porosity is low, such an assumption may not be justifiable. A review of literature shows that rarely is any attention paid to this aspect (thickness and porosity) of the working electrode when making such measurements. Suppose, for example, that concentration polarization is not small at the working electrode, cathode (electrode I). In such a case under an applied voltage, the variation of oxygen partial pressure through electrode I will schematically appear as shown in Fig. 19.[21] In such a case, $\mu^{\mathrm{I}}_{\mathrm{O}_2} < \mu^{\mathrm{II}}_{\mathrm{O}_2}$ where, as before, $\mu^{\mathrm{I}}_{\mathrm{O}_2}$ is the chemical potential of oxygen just outside the interface between electrode I and the electrolyte. In the extreme case, if the porosity is low and/or the electrode thickness is large, the net cathodic current is gas phase diffusion-limited or concentration polarization-limited (through the porous electrode). In such a case, the $p^{\mathrm{I}}_{\mathrm{O}_2}$ reaches some low value, such that beyond some applied

[21] Although in Fig. 19 the variation in p_{O_2} is shown linear, this need not be the case. If there is a gradation in porosity, the variation in p_{O_2} will be nonlinear.

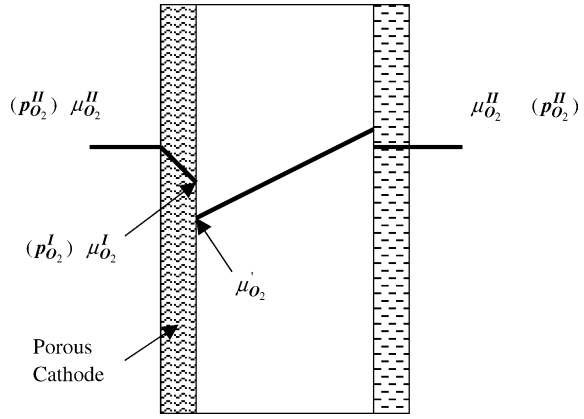

Fig. 19. A schematic variation of oxygen chemical potential, μ_{O_2} (or oxygen partial pressure, p_{O_2}) across a membrane under an applied DC voltage. It is assumed here that concentration polarization is negligible at electrode II. However, at electrode I, it is significant. As a result, there is a variation of μ_{O_2} (and p_{O_2}) through the porous cathode. The variation in p_{O_2} is expected to be approximately linear. In such a case, if $p^{I}_{O_2} \ll p^{II}_{O_2}$, the net flux arriving at the electrode I/electrolyte interface is essentially fixed (concentration polarization limit), and is proportional to $(p^{II}_{O_2} - p^{I}_{O_2}) \approx p^{II}_{O_2}$, beyond some threshold applied voltage. In such a case, the current due to the cathodic reaction, namely $\frac{1}{2}O_2 + 2e' \rightarrow O^{2-}$, is constant, independent of the applied voltage. However, the μ'_{O_2} continues to decrease with increasing applied voltage. If μ'_{O_2} decreases below $\mu^{decomp}_{O_2}$, the electrolyte decomposes resulting in additional (excess) current. If the material exhibits nonstoichiometry, current due to the development of nonstoichiometry can appear before decomposition. Either way, the measured current includes both the cathodic current and that due to decomposition/nonstoichiometry.

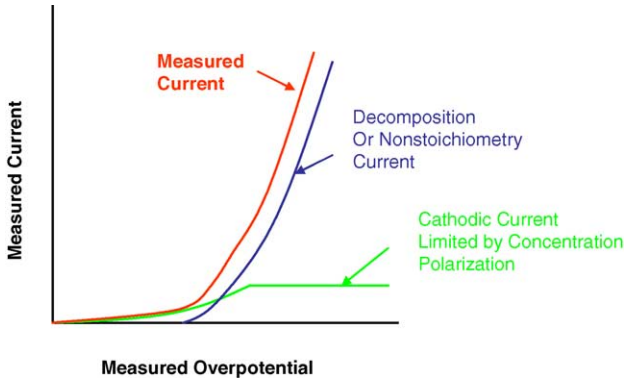

Fig. 20. A schematic illustration of the measured current (—) vs. the measured overpotential using the three-electrode system with significant concentration polarization present. The measured current consists of two contributions: (a) the cathodic current (—), namely, $\frac{1}{2}O_2 + 2e' \rightarrow O^{2-}$, which becomes concentration polarization limited beyond some applied voltage. (b) The decomposition of nonstoichiometry current (—), which begins beyond some applied voltage. The schematic shows both current and overpotential plotted on linear scales. If the current is plotted on a logarithmic scale, the curves will be convex up.

voltage, $p^{I}_{O_2} \ll p^{II}_{O_2}$. In such a case, the cathodic current (due to the cathodic reaction) is fixed. However, if decomposition or nonstoichiometry develops, the measured current will continue to increase with the applied voltage. In such a case, the measured current density, I, versus the measured overpotential, η_m, would have little to do with the actual cathodic reaction. Fig. 20 shows a schematic illustration of the cathodic current, the current due to decomposition/nonstoichiometry, and the measured current as a function of the measured overpotential. From Eq. (78), the minimum applied voltage necessary to effect decomposition is given by

$$\varphi^{II} - \varphi^{I} \approx \left(\frac{\mu^{I}_{O_2} - \mu^{decomp}_{O_2}}{4e}\right)\left(\frac{\ell\rho_i + r'_i + r''_i}{r'_i}\right) + \left(\frac{\mu^{II}_{O_2} - \mu^{I}_{O_2}}{4e}\right) \quad (94)$$

Since

$$\left(\frac{\ell\rho_i + r'_i + r''_i}{r'_i}\right) > 1$$

it is clear that $\Delta\varphi = \varphi^{II} - \varphi^{I}$, the applied voltage necessary to cause decomposition given by Eq. (94), is lower than that given by Eq. (92). That is, if significant concentration polarization exists at the working electrode, the decomposition (or the development of nonstoichiometry) will occur at a lower voltage. If, however, $r'_i \gg r''_i$ and $r'_i \gg \ell\rho_i$, then Eq. (94) reduces to Eq. (93). Several cases can be examined corresponding to various relative values of transport parameters, and the details will albeit vary. However, the important conclusion is the same, namely that in the three-electrode system under an applied DC voltage, current due either to the development of nonstoichiometry in the electrolyte or due to electrolyte decomposition can occur, in addition to the current due to the cathodic reaction. The intended purpose of the three-electrode system is to investigate electrode kinetics, i.e., to investigate relationship between cathodic overpotential and the current due to the cathodic reaction, namely $\frac{1}{2}O_2 + 2e' \rightarrow O^{2-}$. The net measured current, however, will most likely include two contributions: current due to the cathodic reaction and current due to the occurrence of decomposition/nonstoichiometry. It is possible that under certain conditions the current due to decomposition/nonstoichiometry may completely overwhelm the cathodic current. In such cases, the three-electrode system will result in significant overestimation of cathodic electrocatalytic activity, and may not be a reliable technique, especially at high, applied voltages, and when the material readily develops nonstoichiometry—such as ceria. It can be shown experimentally that current due to nonstoichiometry/electrolyte decomposition can be several times that due to the cathodic reaction under relatively modest applied voltages [22].

3. Discussion

The main objective of this manuscript was to develop transport equations through mixed oxygen ion and electronic conducting membranes, and through predominantly oxygen ion conducting membranes, by incorporating transport across

interfaces. The analysis assumes the usual criteria of local equilibrium and electroneutrality. As emphasized, the assumption of local equilibrium implies that electronic current cannot be assumed to be identically zero,[22] even in a predominantly oxygen ion conductor, such as zirconia. This has important implications concerning the chemical potential of oxygen in the membrane, and thus the very stability of the membrane. It is well known that many factors dictate transport through membranes and across interfaces, and the assumption of transport parameters as constants (independent of oxygen partial pressure) is an oversimplification. At the same time, however, such a simplification is deemed necessary in order to elucidate the fundamental phenomena in a simple analytical framework, which is not possible if one incorporates the dependence of transport parameters on defect chemistry and on local p_{O_2}.[23] If the exact dependencies of transport parameters on p_{O_2} (or μ_{O_2}) are known for a given material and interfacial regions, which is rarely the case, numerical solutions to transport equations can be readily developed. Such an approach was not chosen here, as the purpose was to focus on fundamental aspects of transport, with emphasis on interfaces, and not on any specific material with any particular defect structure. In this framework, three cases were examined: (1) MIEC oxygen separation, (2) fuel cells, and (3) voltage-driven oxygen separation.

For the case of MIEC oxygen separation, it was shown that the μ_{O_2} always varies through the membrane monotonically between the two end values (corresponding to the two atmospheres), regardless of the nature and the details of interfacial processes. This has important implications concerning the thermodynamic stability of the membrane. The analysis shows that to ensure membrane stability, it is necessary that $\mu''_{O_2} > \mu^{\text{decomp}}_{O_2}$, a condition which could be achieved even if $\mu^{\text{II}}_{O_2} < \mu^{\text{decomp}}_{O_2}$. Thus, the implication is that if a membrane is used for the production of syngas, for example, it is necessary to ensure that $\mu''_{O_2} > \mu^{\text{decomp}}_{O_2}$. That is, the transport properties, especially across interfaces, must be so adjusted to ensure that $\mu''_{O_2} > \mu^{\text{decomp}}_{O_2}$. The exact variation of μ_{O_2} through the membrane depends upon the various transport parameters, including those of interfaces. This implies that one may need to deposit a thin (a few nanometers) layer of some material of appropriate transport properties on the permeate side to ensure stability of an otherwise unstable membrane in the imposed atmosphere. The same general conclusions apply to fuel cells. That is, depending upon electrode effects, an otherwise unstable electrolyte may exhibit stability in fuel. It is known, for example, that a fuel cell made with phase-stabilized cubic or rhombohedral Bi_2O_3 readily decomposes to metallic bismuth in hydrogen as fuel. However, it has been observed that the same fuel cell remains stable when operated in lightly humidified (∼3% H_2O) methane, even when the μ_{O_2} in the fuel is lower than $\mu^{\text{decomp}}_{O_2}$ [23]. This suggests that electrode characteristics must be such that with methane as a fuel, μ''_{O_2} must be greater than $\mu^{\text{decomp}}_{O_2}$, that is $\mu''_{O_2} > \mu^{\text{decomp}}_{O_2}$, even when $\mu^{\text{II}}_{O_2} < \mu^{\text{decomp}}_{O_2}$. A possible approach to preventing decomposition of bismuth oxide based electrolyte is the deposition of a more stable material such as YSZ or rare earth oxide-doped ceria, such as samaria-doped ceria (SDC), on the side exposed to fuel. By suitably tailoring the properties and thicknesses of the two regions, analysis based on bulk transport suggests that it may be possible to prevent electrolyte decomposition by ensuring that the μ_{O_2} in bismuth oxide never goes below the corresponding $\mu^{\text{decomp}}_{O_2}$ [14]. However, the required thickness of YSZ or SDC to prevent decomposition is often comparable to or may even be much greater than that of bismuth oxide, which defeats the very purpose of using a high conductivity bismuth oxide based electrolyte [14,24]. The present work suggests that a more profitable approach may involve modification of the anode/electrolyte interface. This, for example, could be the case III from Fig. 7, where $r''_e \gg r_e, r'_e$. Thus, the present work suggests a possible approach for using Bi_2O_3-based electrolytes by suitably modifying the anode/electrolyte interface.

For fuel cells, equations for electrode overpotentials in terms of ionic and electronic current densities, and interfacial transport parameters were developed. The usual definition of overpotential is as a measure of the loss of useful voltage in irreversible processes. From the standpoint of thermodynamics, however, the overpotential loss should strictly be described in terms of the rate of loss of potential work (which can be derived as decrease in free energy) into heat. The usual approach is to describe the overpotential as a measurable voltage loss, as a function of current (measured in the external circuit). The inclusion of internal electronic leakage, when the overpotential loss is given as a measure of the potential work degraded as heat, leads to the conclusion that at OCV, the overpotential, defined as the rate of loss of potential work at an electrode divided by the measured current, is actually infinite. This is because even when no current is flowing in the external circuit, part of the potential work is continually being degraded as heat due to internal electronic leakage. As stated earlier, the electronic current can never be zero when potential gradients exist, with the result that at OCV, the as-defined overpotential is singular—or infinite. Also, the overpotential as-defined may not be measurable. At the same time, however, the relevant physical parameter is the product of the as-defined overpotential and current, which is always finite, and is a measure of the rate of degradation of potential work into heat (an irreversible process). In a typical practical

[22] Unless shorted externally.

[23] There are many published reports, which have incorporated the defect chemistry details into the analysis. However, this necessitated making simplifying assumptions regarding the thermodynamics of defects. Also, in so doing, the important features of electron transport across interfaces were generally overlooked. This not only leads to incomplete description of transport, but also does not permit the estimation of μ_{O_2} inside the membrane, unless further simplifying assumptions are made about μ_{O_2} variation across interfaces. For example, Eq. (31) can explicitly give $\mu_{O_2}(x)$ when it is assumed that $\mu'_{O_2} = \mu^{\text{I}}_{O_2}$ and $\mu'_{O_2} = \mu^{\text{II}}_{O_2}$, an assumption which is rarely justified.

case wherein the electronic leakage is usually negligible, and a finite current flows through the external circuit (such that $|I_L| \approx |I_i| \gg |I_e|$), the overpotential defined here is essentially the same as the usual one, and measured experimentally.

In both MIEC oxygen separation membranes and fuel cells, the μ_{O_2} and φ are interrelated. In voltage-driven oxygen separation systems, however, both μ_{O_2} and φ can be independently varied, which implies an additional (experimental) degree of freedom. In such a case, the μ_{O_2} in the membrane can lie outside of the end values. That is, $\mu_{O_2}^{\text{membrane}}$, can be greater or lower than $\mu_{O_2}^{\text{I}}$ and/or $\mu_{O_2}^{\text{II}}$. Transport parameters of the membrane and across interfaces, and the applied voltage determine the actual variation of μ_{O_2} in the membrane. Figs. 12–15 show the various possibilities. An important point to note is that by virtue of the fact that $\mu_{O_2}^{\text{membrane}}$ can lie outside of the end values implies that it is possible for $\mu_{O_2}^{\text{membrane}}$ to be lower than $\mu_{O_2}^{\text{decomp}}$. Under such conditions, localized membrane decomposition or nonstoichiometry can occur. This has important implications concerning the use of the so-called three-electrode system under an applied DC voltage for the measurement of electrode polarization behavior. The analysis shows that in the three-electrode system, a significant contribution to the net measured current can occur from membrane decomposition (or the development of nonstoichiometry), leading to an inadvertent overestimation of electrode electrocatalytic activity. The present work thus shows that caution should be exercised in using the three-electrode system under an applied DC bias for the investigation of electrocatalytic activity of an electrode. It is also possible that the μ_{O_2} in the membrane may be much greater than both $\mu_{O_2}^{\text{I}}$ and $\mu_{O_2}^{\text{II}}$ under an applied DC voltage. In such a case, cracking of the membrane can occur under an applied DC voltage, as has been previously shown theoretically and experimentally [15,16].

All transport equations are given under the simplifying assumption that transport properties are independent of μ_{O_2}, which allows one to obtain simple analytical equations. At the same time, the fact that the chemical potential of oxygen is a function of position, $\mu_{O_2}(x)$, implies that small changes in composition are presumed to occur until steady state is established. The net integrated oxygen flux arriving or leaving an elemental region dx is directly related to the interrelationship between composition (stoichiometry) and μ_{O_2}. If for a given change in μ_{O_2}, namely $\Delta\mu_{O_2}$, the change in composition is small (narrow stoichiometry range), this means the capacity of the internal EMF will also be small. If chemical capacitors are used to describe the equivalent circuit, then it will imply that the magnitude of the chemical capacitance is small. This may likely be the case with zirconia. Alternatively, if for a given change in μ_{O_2}, namely $\Delta\mu_{O_2}$, the change in composition is large (wide stoichiometry range), this means the capacity of the internal EMF will also be large. If chemical capacitors are used, then it will imply that the magnitude of the chemical capacitance is large. This may likely be the case with ceria. Regardless of whether internal EMF or chemical capacitors are used, it is clear that a complete description of transport will require relationship between composition (stoichiometry) and μ_{O_2}, which will most likely have to be determined experimentally. Unfortunately, this is rarely known for any material with any degree of certainty.

4. Summary

In the present manuscript equations were developed to describe transport of oxygen ions and electrons through membranes by explicitly taking into account interface properties. The fundamental assumptions made are the same as in virtually all of the earlier studies, namely, the existence of electroneutrality and local equilibrium. The assumption of local equilibrium is shown to imply that electronic current cannot be entirely neglected, however small, to ensure that local chemical potential of oxygen, μ_{O_2}, is uniquely defined. That is, even in a predominantly oxygen ion conductor, electronic transport must be taken into account. Transport of oxygen ions and electrons through the membrane as well as across electrode/membrane interfaces was taken into account in the present work. These equations were then applied to fuel cells, MIEC oxygen separation membranes under an applied pressure gradient, voltage-driven oxygen separation, and the three-electrode system which is often used for the study of electrode kinetics. It was shown that in fuel cells or MIEC oxygen separation membranes, as long as the chemical potential of oxygen on the reducing side (anode in the case of fuel cells; permeate side for MIEC oxygen separation or fuel side for the synthesis of syngas using MIEC membranes) is greater than the chemical potential of oxygen corresponding to membrane thermodynamic stability, membrane decomposition should not occur. Membrane may continue to be stable even if the chemical potential of oxygen in the anode gas (fuel cells) or permeate side (MIEC membranes) is lower than the decomposition chemical potential, provided the interface transport properties are suitably tailored such that the chemical potential of oxygen just inside the interface is greater than the decomposition chemical potential, that is $\mu''_{O_2} > \mu_{O_2}^{\text{decomp}}$. However, in the case of oxygen separation under the action of an applied voltage, depending upon the magnitude of the applied voltage and the relative transport parameters of the membrane and interfacial regions, the chemical potential of oxygen in the membrane inside the interfaces can go below the decomposition chemical potential. In such a case, membrane decomposition can occur, or a nonstoichiometry may develop. This has significant implications concerning the use of the so-called three-electrode system for the study of electrode kinetics, for example for the study of a prospective cathode for SOFC. The significance is that measurements made using the three-electrode system under high applied voltages may yield erroneous conclusions concerning cathode activity, since the net current generated will consist of two terms: (a) that due to the actual cathodic reaction, namely $\frac{1}{2}O_2 + 2e' \rightarrow O^{2-}$, and (b) that due to the occurrence of decomposition and/or

the development of nonstoichiometry (oxygen deficiency). In a typical experiment, the measured current is invariably attributed to the cathodic reaction, thereby overestimating the cathodic activity of the prospective cathode, since the experimenter has no way of separating the two. In many cases, the current due to nonstoichiometry/decomposition may be much larger than the cathodic current, leading to large errors in the estimation of cathodic activity. The analysis also shows that the decomposition (or the development of oxygen deficiency) may occur just under the positive electrode or just under the negative electrode, depending upon the relative magnitudes of ionic and electronic transport parameters of the bulk and the interfaces. In practice, however, the occurrence of decomposition (or the development of oxygen deficiency) under the positive electrode is deemed unlikely. This is because in such a case, the electrons required for the neutralization of the cation (Zr^{4+} to Zr) transport through the membrane, which may be kinetically hindered if the electronic conductivity is low. Decomposition (or the development of oxygen deficiency) under the positive electrode, however, is likely in the case of ceria-based membranes under appropriate conditions since electronic conductivity of ceria is typically much higher, especially at low p_{O_2}.

All transport equations are given in a general form, without invoking any particular defect structure. The rationale is that fundamental stability issues are not dependent on the types and nature of defects. All transport equations are given assuming transport parameters to be independent of μ_{O_2}. Because of this assumption, the spatial variations of μ_{O_2}, φ, and $\tilde{\mu}_{O^{2-}}$ through the membrane are shown to be linear. This assumption also allows the use of simple equivalent circuits. Bulk regions were modeled using a combination of ionic and electronic area specific resistances for the bulk and an internal EMF source. Interfacial regions were also modeled using internal EMF sources, instead of capacitors, in combination with ionic and electronic area specific resistances. This is entirely consistent with the definition of Nernst voltage in terms of the net $\Delta\mu_{O_2}$ across an interface. As such, its modeling as an EMF source is equally appropriate, and in fact, is more consistent with the general thermodynamic framework. Usually the transport parameters are μ_{O_2}-dependent. In such cases, the variation of μ_{O_2}, φ, and $\tilde{\mu}_{O^{2-}}$ will not be spatially linear. If the dependencies for a given material and interfacial regions are precisely known, which is rarely the case, the spatial variations of μ_{O_2}, φ, and $\tilde{\mu}_{O^{2-}}$ can be easily evaluated numerically—if not analytically. Such an approach was not selected here. The simplification made may only alter the details, but not the broader, general conclusions.

Acknowledgements

This work was supported by the U.S. Department of Energy under contract no. DE-FC26-02NT41602.

References

[1] M.H. Hebb, J. Chem. Phys. 20 (1952) 185.
[2] L. Heyne, Mass Transport in Oxides, NBS Special Publication 296, 1968, pp. 149–164.
[3] C. Wagner, Prog. Solid-State Chem. 10 (1) (1975) 3–16.
[4] H. Rickert, Electrochemistry of Solids: An Introduction, Springer-Verlag, Berlin, 1982.
[5] H. Schmalzried, Chemical Kinetics of Solids, VCH Publication, Weinheim, 1995.
[6] N.S. Choudhury, J.W. Patterson, J. Electrochem. Soc. 118 (9) (1971) 1398–1403.
[7] D.S. Tannhauser, J. Electrochem. Soc. 125 (8) (1978) 1277–1282.
[8] I. Riess, J. Electrochem. Soc. 128 (10) (1981) 2077–2081.
[9] S. Yuan, U.B. Pal, J. Electrochem. Soc. 143 (10) (1996) 3214–3222.
[10] H. Nafe, J. Electrochem. Soc. 144 (11) (1997) 3922–3929.
[11] R. Singh, K.T. Jacob, J. Appl. Electrochem. 33 (2003) 571–576.
[12] D. Kondepudi, I. Prigogine, Modern Thermodynamics, Wiley, New York, 1998.
[13] R.D. Armstrong, M. Todd, in: P.G. Bruce (Ed.), Solid State Chemistry, Cambridge University Press, Cambridge, UK, 1995.
[14] A.V. Virkar, J. Electrochem. Soc. 138 (5) (1991) 1481–1487.
[15] A.V. Virkar, J. Mater. Sci. 20 (1985) 552–562.
[16] A.V. Virkar, J. Nachlas, A.V. Joshi, J. Diamond, J. Am. Ceram. Soc. 73 (11) (1990) 3382–3390.
[17] P. Kofstad, High-temperature Oxidation of Metals, Wiley, New York, 1966.
[18] J.R. Macdonald, Impedance Spectroscopy, A Wiley-Interscience Publication, Wiley, New York, 1987.
[19] M. Liu, H. Hu, J. Electrochem. Soc. 143 (6) (1996) L109.
[20] V.V. Kharton, F.M.B. Marques, Solid State Ion. 140 (2001) 381–394.
[21] H. Matsumoto, S. Hamajima, T. Yajima, H. Iwahara, J. Electrochem. Soc. 148 (10) (2001) D121–D124.
[22] A.V. Virkar, Y. Jiang, Submitted to Proceedings of the SOFC-IX, Electrochemical Society, 2005.
[23] W. Lawless, Private communication, 2003.
[24] J.-Y. Park, E.D. Wachsman, in: S.C. Singhal, M. Dokiya (Eds.), Proceedings of the Eighth International Symposium SOFC VIII, Electrochemical Society, Pennington, NJ, 2003, pp. 289–298.